



# Toward Wireless Control in Industrial Process Automation

## A CASE STUDY AT A PAPER MILL

ANDERS AHLÉN,  
JOHAN ÅKERBERG,  
MARKUS ERIKSSON,  
ALF J. ISAKSSON,  
TAKUYA IWAKI,  
KARL HENRIK JOHANSSON,  
STEFFI KNORN,  
THOMAS LINDH,  
and HENRIK SANDBERG

**W**ireless sensors and networks are used only occasionally in current control loops in the process industry. With rapid developments in embedded and high-performance computing, wireless communication, and cloud technology, drastic changes in the architecture and operation of industrial automation systems seem more likely than ever. These changes are driven by ever-growing demands on production quality and flexibility. However, as discussed in “Summary,” there are several research obstacles to overcome. The radio communication environment in the process industry is often troublesome, as the environment is frequently cluttered with large metal objects, moving machines and vehicles, and processes emitting radio disturbances [1], [2]. The successful deployment of a wireless control system in such an environment requires careful design of communication links and network protocols as well as robust and reconfigurable control algorithms.

Digital Object Identifier 10.1109/MCS.2019.2925226  
Date of publication: 16 September 2019



COURTESY OF IGGESUND PAPERBOARD; PHOTO: STEFFI KNORR

Based on examples from the Iggesund Mill in Sweden (see “Iggesund Mill History”), this article discusses some recent developments in wireless control in industrial process automation. Despite major scientific progress over the past couple of decades in wireless networked control [3] (including important results on how plants can be stabilized and optimized over packet-switched networks [4]), surprisingly, there has been little impact on commercial implementations in the process industry. We argue that a more integrated approach to the design of these systems is needed and explore systematic tradeoffs between the communication and control systems. Existing standardized industrial communication protocols (ISA-100 and WirelessHART) provide a large degree of freedom for users, including many tuning parameters. However, co-design methods using this freedom are still needed [5]. A brief survey of recent advances in wireless control is presented in “Advances in Wireless Control.”

The outline of this article is as follows. First, a possible future control architecture is described, and key challenges in next-generation process automation are detailed. The Iggesund paper mill is then introduced as a case study that is used throughout the article to illustrate the considered communication and control problems. Results are presented on modeling radio channels in an industrial environment. The joint behavior of multiple wireless sensor–sensor and sensor–gateway (GW) channels is discussed, and models useful for routing data packets are proposed. Energy harvesting in wireless sensor networks is then demonstrated on the industrial process. Event-based control of wireless systems is investigated for both feedback and feedforward control, followed by a proof-of-concept implementation of wireless control at Iggesund. Finally, conclusions are drawn.

## CHALLENGES IN NEXT-GENERATION PROCESS CONTROL

With the recent developments in the Internet of Things, future devices and systems are expected to communicate much more seamlessly. The most immediate effects are seen in data analytics, where new devices collect data online and feed them into the cloud without going through a control system. Once in the cloud, almost unlimited computing power can be applied to processing the data for various purposes (predictive or prescriptive maintenance). It is clear

that this will have an effect not only on analytics but also on process control and other process operations.

Inspired by the development in mobile platforms (iPhone and Android), it is reasonable to assume that most functions that are not time or safety critical could become available as apps in an automation platform. Presently, there are often large monolithic software systems for each layer of the classical automation pyramid (for process control, manufacturing execution system, and enterprise resource planning). Instead, these functions may be decomposed into smaller components that seamlessly communicate within one app platform. This would also make it easier for smaller players, which only provide a limited or smaller scope of functionality, to participate in the market.

As one of the world’s largest process companies, ExxonMobil clearly communicated its vision toward a future control architecture in 2016 [6]. Its vision states concretely that a future control system should be built on distributed control nodes (DCNs) that are dedicated single-channel, input–output modules with control capability connected to a real-time data service bus. Furthermore, the operations platform should be open and use open source software. This would enable a much easier revamping of current distributed control system (DCS) architecture philosophy, which, in ExxonMobil’s view, is both complex and expensive. By adopting this vision, together with the idea of a common app platform, the traditional automation pyramid (which structurally separates process control, scheduling, and planning into their own hierarchical levels) may be replaced by a more flexible paradigm. A somewhat simplified version of the ExxonMobil vision is depicted in Figure 1.

At the lowest level of a control system are measurement devices (sensors and analyzers) and actuating devices (valves

## Summary

**W**ireless sensor networks are, to a growing extent, being deployed in the process industry. However, there are still several issues that must be addressed for this technology to reach its full potential. This article describes the main challenges in next-generation process control, with an architecture based on distributed control nodes connected to a real-time data bus over wireless and wired networks. A case study, focused on one of the starch cooker processes of the Iggesund Mill in Sweden, was used to illustrate various challenges and solutions to sensing, communication, and control for emerging wireless process automation. Radio environment modeling, network protocol design, energy harvesting, and event-based control are discussed in detail. Experimental tests on the starch cooker during normal production over five consecutive days indicate that it is sometimes possible to replace wired control systems with wireless in complex industrial environments.

and pumps). At this device level, the connection to the common real-time bus could be realized through a standardized DCN, as suggested by ExxonMobil. It is more futuristic, however, to assume that all devices have enough intelligence to handle the connectivity and low-level control

computations themselves [7]. As previously indicated, one interesting question is where a particular computation should occur. Clearly, there will always be a need to execute some computations with a minimal latency. Hence, a tradeoff exists between moving current DCS functionality to the

## Iggesund Mill History

Iggesund Mill's origin is in the forests outside Hudiksvall in Sweden, in the small town of Iggesund. The area has a long history; there were already small industries in and around the town in the middle of the 16th century. In 1685, trader and chief commissioner Isak Breant received a license to construct an ironworks in the lower part of Iggesundån (Iggesund River). Soon thereafter, production began at the plant.

However, in the upper part of Iggesundån, there was already a paper mill (Östanå Mill). Iggesund Mill bought this mill in 1771. Östanå Mill was the first in the world to try to produce paper from sawdust and wood. However, it never passed the experimental stage, and in 1842, the paper mill burned down.

In 1869, Baron Gustav Tamm took over as owner of Iggesund Mill and was able to construct a large sawmill, which he started building in 1870. In addition to the purchase of Östanå Mill, this marks the first transition from a refined iron industry to wood industry. From 1915 to 1917, a cellulose factory was built on a new site further away from Iggesundån (see Figure S1 and S2). In 2017, the company celebrated the fact that the factory had remained in the same location for 100 years.

Today, Iggesund Mill is best known for its white premium cardboard (Figure S3). However, it was not until the beginning of the 1960s that the mill started making it. Iggesund Mill was

only the third manufacturer in the world to install a carton machine using modern technology; the other two were in Australia and England. In 1963, the first cardboard machine at the Iggesund Mill began operation; the second machine started in 1971.



**FIGURE S2** An aerial view of Iggesund Bruk from 1940. At that time, Iggesund Bruk was only a pulp mill. The first cardboard machine was started in 1963, and with this, Iggesund Bruk became both a producer of pulp and cardboard. The factory is still in the same location where the first pulp mill opened in 1916. (Source: Iggesund Paperboard; used with permission.)

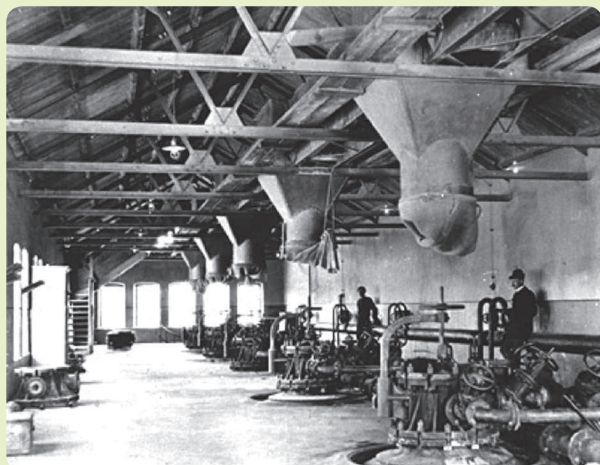


**FIGURE S1** The production room of the old sulphite digester. The house has long been demolished, and today there are no traces remaining of it. At the time of photo (1916), the sulphite process was used to produce pulp. Today, the process has changed to use the sulphate process to achieve a better quality and whiteness of the pulp. (Source: Iggesund Paperboard; used with permission.)



**FIGURE S3** Iggesund Paperboard's first cardboard machine (KM1) is still in use. However, it has been rebuilt several times since the photo was taken in 1968. The photo shows the reeling of the cardboard, and coating stations are in the middle of the picture. At the far left, the cardboard machine's drying unit is visible. (Source: Iggesund Paperboard; used with permission.)

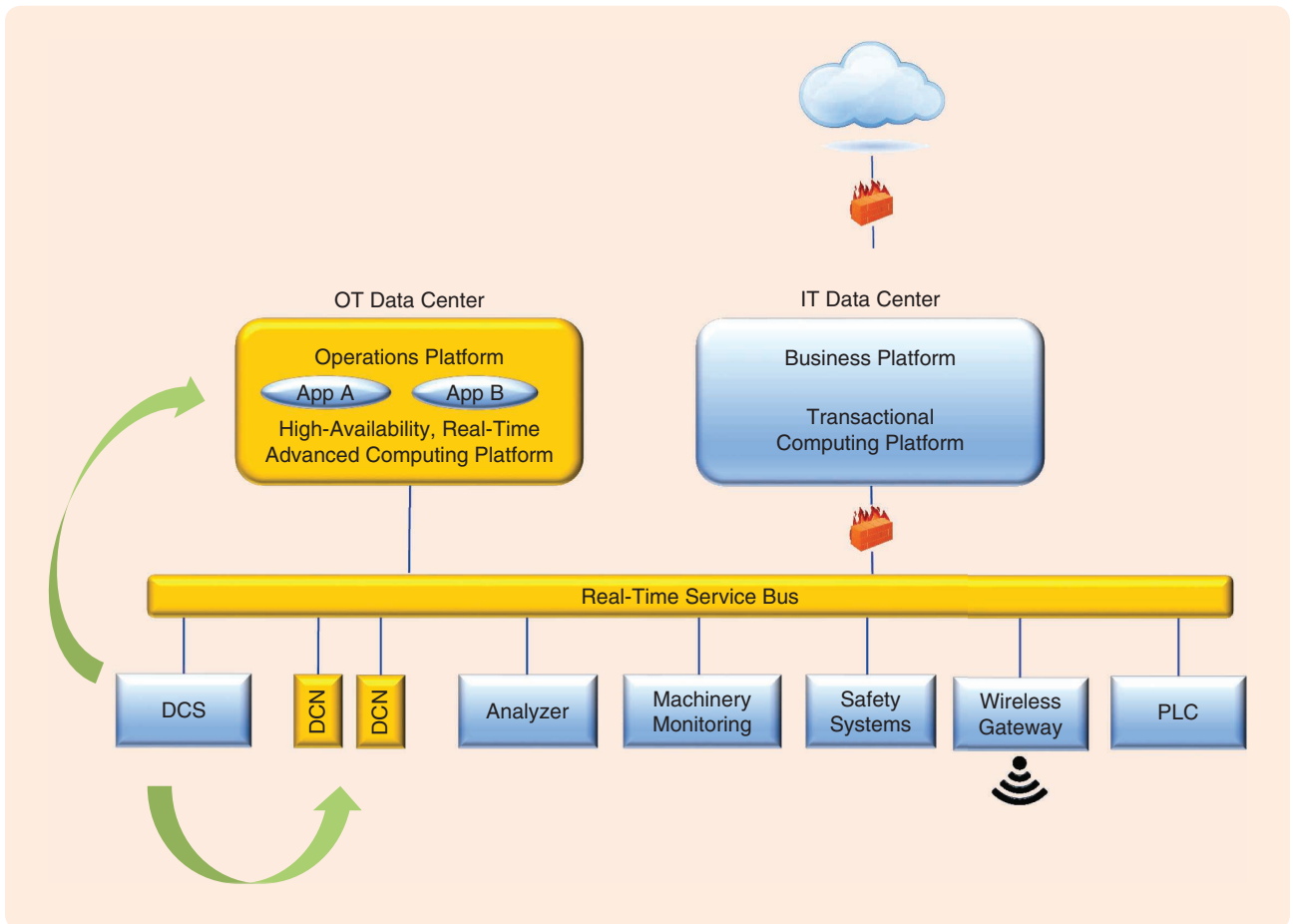


**FIGURE 1** The layout of a future control architecture. The system contains distributed control nodes (DCNs) (used as dedicated single-channel, input–output modules) with control capability. Through a real-time data service bus, the modules are connected to the operations open platform running open source software. This setup, together with a common app platform, is expected to replace the traditional automation pyramid that structurally separates process control, scheduling, and planning to their own hierarchical levels. This leads to a more flexible and cost-effective paradigm. DCS: distributed control system; OT: operational technology; PLC: programmable logic controller. (Image used with permission from ExxonMobil.)

operations platform or the DCN/device, as indicated by the arrows in Figure 1.

A central question in this article is what role wireless communications will play in this future automation architecture. In Figure 1, the possibility of a wireless GW is indicated. However, we argue that a standard choice for the DCNs and other intelligent devices would be to use wireless communications, even for situations requiring fast communications. As noted by others [2], [8], [9], there are multiple potential advantages with wireless compared to wired communications, including cost savings in cables and installation and more flexible operation. This article investigates the feasibility and reliability of wireless communications in process applications, with a specific focus on the pulp and paper industry.

From a system perspective, there are also several challenges to maintain high availability and safe control functions. From an engineering perspective, the control applications must support online changes, and the system



**FIGURE 2** The Iggesund Mill, which is part of the Holmen group. The small community in Iggesund is located on the coast of the Bothnian Sea, on Sweden's east coast. The mill produces one of the world's leading paperboard brands, Invercote. Approximately 700 people work in the mill, and the factory produces approximately 420,000 tons of pulp and 330,000 tons of cardboard every year. (Source: Iggesund Paperboard; used with permission.)

architecture must address seamless reconfiguration (distributing new applications while ensuring system integrity). Furthermore, on the real-time bus, new challenges arise to address different real-time traffic classes, video streams, and best-effort traffic in a system architecture, as shown in

Figure 1. In addition, redundancy is required to meet the industry demand for the availability of the control system (and to take the processes into safe states in case of errors that cannot be automatically recovered), without creating isolated network functions that are executing (partly) blindly.

## Advances in Wireless Control

Along with the development of wireless technology, industrial control by means of wireless communications has received much attention in both academia and industry. Recent research issues on control over wireless communications, especially in industrial automation systems, are summarized in [2], [5], [9], and [S1]–[S4]. In [5], [S1], and [S2], communication protocols developed for industrial wireless communications (WirelessHART [S5] and ISA-100 [S6]) are discussed. In both WirelessHART and ISA-100, hardware and protocols are specified by the standard of the low-rate wireless personal area network, IEEE 802.15.4 [S7]. Some research focuses on the implementation and design of control systems operating over the WirelessHART and ISA-100 communication protocols. In [S8], aperiodic control algorithms implemented over the IEEE 802.15.4 standard are proposed and evaluated on a double-tank laboratory experimental setup. A network model that captures important key aspects of the WirelessHART protocol—a multihop structure and time-division multiple access communications with different frequencies—is developed in [S9] and [S10]. Emulation-based stability conditions are derived in [S9], and observer design under the impact of stochastic noise is discussed in [S10]. A model of control systems over a multihop network is proposed in [S11]. Based on this model, a co-design framework comprising both controller and network scheduling and routing is investigated in [S12]. In [S13], a co-design of linear-quadratic-Gaussian (LQG) control and multihop network scheduling and routing and its reconfiguration is discussed. In [S14], a co-design of controller and network scheduling and routing is proposed for the WirelessHART standard, which is assumed to have network reconfiguration after a given period.

Wireless control is also studied in the context of networked control theory, which, in general, focuses on control problems under network-induced constraints—delay, packet dropout, and channel capacity limitation [4], [S15]–[S17]. In [S18], LQG control with packet dropouts is considered. In [S19], a network with multiple sensors is examined, while communication through intermediate nodes is studied in [S20]. LQG control with network-induced delays and access constraints is investigated in [S21] and [S22], where only a subset of sensors can access the controller. Network capacity is explicitly considered as a control- and information-theory problem in [S23]–[S25].

The scheduling of data transmission of networked control systems has attracted attention to reduce the amount of communication. In [S26] and [S27], a joint optimization problem is

presented, where the problem can be separated into optimal estimation, control, and scheduling. Scheduling among multiple control loops with a shared communication network is proposed in [S28] and [S29]. A prioritizing framework under limited channel slots is proposed in [S28], and a scheduling framework under a media-access-control-like protocol is developed in [S29]. There is significant research considering sensor scheduling for state estimation. In [S30], a communication control scheme for Kalman filters is developed to improve the tradeoff between estimation performance and communication cost. Optimal estimation with a multiple time-step cost is introduced in [S31]. The minimum mean-square error (MMSE) estimation schedule can be obtained in special cases. In [S32], the MMSE schedule between two sensors is obtained, which is extended to more sensors in [S33] and [S34]. These works address a single-hop network, that is, every sensor can directly communicate with the remote estimator. A multihop network structure is considered in [S35]–[S37]. In [S36] and [S37], how to manage the control systems when the network environment is changed is considered. In [S36], a way to reconfigure the network under time-varying channel states is proposed.

Energy-aware control strategies over wireless communication are investigated in previous work. Optimal sensor energy allocation is studied in [S38]–[S40]. Therein, the energy consumption is dealt with as a control variable, which determines the probability of packet loss. Energy allocation for state estimation is discussed in [S38] and [S40]–[S41] and for optimal control in [S39]. Network control systems with energy-harvesting sensors are considered in [S43]–[S45].

## REFERENCES

- [S1] J. R. Moyne and D. M. Tilbury, "The emergence of industrial control networks for manufacturing control, diagnostics, and safety data," *Proc. IEEE*, vol. 95, no. 1, pp. 29–47, 2007.
- [S2] C. Lu et al., "Real-time wireless sensor-actuator networks for industrial cyber-physical systems," *Proc. IEEE*, vol. 104, no. 5, pp. 1013–1024, 2016.
- [S3] A. Willig, K. Matheus, and A. Wolisz, "Wireless technology in industrial networks," *Proc. IEEE*, vol. 93, no. 6, pp. 1130–1151, 2005.
- [S4] A. A. Kumar S. K. Øvsthus, and L. M. Kristensen, "An industrial perspective on wireless sensor networks: A survey of requirements, protocols, and challenges," *IEEE Commun. Surveys Tuts.*, vol. 16, no. 3, pp. 1391–1412, 2014.
- [S5] D. Chen, M. Nixon, and A. Mok, *WirelessHART: Real-Time Mesh Network for Industrial Automation*. New York: Springer-Verlag, 2010.
- [S6] *Wireless Systems for Industrial Automation: Process Control and Related Applications*, ISA-100.11a, 2009.
- [S7] *Wireless Medium Access Control (MAC) and Physical Layer (PHY) Specification for Low-Rate Wireless Personal Area Networks (WPANs)*, IEEE 802.15.4. 2019. [Online]. Available: <http://www.ieee802.org/15/pub/TG4.html>

## THE IGGESUND PAPERBOARD MACHINE CASE STUDY

The Iggesund Mill is a fully integrated pulp and paperboard mill with a long history (see “Iggesund Mill History”). In Figure 2, the pulp mill is located in the area by

the large chimneys in the back of the photo; the paperboard mill and the coating kitchen are the building complex in the middle of the figure. There are two paperboard machines (see Figure 3), and the products manufactured there are primarily for packaging and graphic purposes

- [S8] J. Araújo, M. Mazo, A. Anta, P. Tabuada, and K. H. Johansson, “System architectures, protocols and algorithms for aperiodic wireless control systems,” *IEEE Trans. Ind. Informat.*, vol. 10, no. 1, pp. 175–184, 2014.
- [S9] A. I. Maass, D. Nešić, R. Postoyan, P. M. Dower, and V. S. Varma, “Emulation-based stabilisation of networked control systems over wirelessHART,” in *Proc. IEEE Conf. Decision and Control*, 2017, pp. 6628–6633.
- [S10] A. I. Maass, D. Nešić, R. Postoyan, and P. M. Dower, “Observer design for networked control systems implemented over WirelessHART,” in *Proc. IEEE Conf. Decision and Control*, 2018, pp. 2836–2841.
- [S11] R. Alur, A. D’Innocenzo, K. H. Johansson, G. J. Pappas, and G. Weiss, “Compositional modeling and analysis of multi-hop control networks,” *IEEE Trans. Autom. Control*, vol. 56, no. 10, pp. 2345–2357, 2011.
- [S12] F. Smarra, A. D’Innocenzo, and M. D. Di Benedetto, “Optimal co-design of control, scheduling and routing in multi-hop control networks,” in *Proc. IEEE Conf. Decision and Control*, 2012, pp. 1960–1965.
- [S13] T. Iwaki and K. H. Johansson, “LQG control and scheduling co-design for wireless sensor and actuator networks,” in *Proc. IEEE Workshop Signal Processing Advances in Wireless Communications*, 2018. doi: 10.1109/SPAWC.2018.8445965.
- [S14] G. D. Di Girolamo and A. D’Innocenzo, “Codesign of controller, routing and scheduling in wirelessHART networked control systems,” *Int. J. Robust Nonlin.*, vol. 29, no. 7, pp. 2171–2187, 2019.
- [S15] W. Zhang, M. S. Branicky, and S. M. Phillips, “Stability of networked control systems,” *IEEE Control Syst. Mag.*, vol. 21, no. 1, pp. 84–99, 2001.
- [S16] L. Schenato, B. Sinopoli, M. Franceschetti, K. Poolla, and S. S. Sastry, “Foundations of control and estimation over Lossy networks,” *Proc. IEEE*, vol. 95, no. 1, pp. 163–187, 2007.
- [S17] W. M. H. Heemels, A. R. Teel, N. Van de Wouw, and D. Nesic, “Networked control systems with communication constraints: Tradeoffs between transmission intervals, delays and performance,” *IEEE Trans. Autom. Control*, vol. 55, no. 8, pp. 1781–1796, 2010.
- [S18] V. Gupta, B. Hassibi, and R. M. Murray, “Optimal LQG control across packet-dropping links,” *Syst. Control Lett.*, vol. 56, no. 6, pp. 439–446, 2007.
- [S19] V. Gupta, N. C. Martins, and J. S. Baras, “Optimal output feedback control using two remote sensors over erasure channels,” *IEEE Trans. Autom. Control*, vol. 54, no. 7, pp. 1463–1476, 2009.
- [S20] V. Gupta, A. F. Dana, J. P. Hespanha, R. M. Murray, and B. Hassibi, “Data transmission over networks for estimation and control,” *IEEE Trans. Autom. Control*, vol. 54, no. 8, pp. 1807–1819, 2009.
- [S21] D. Hristu-Varsakelis and L. Zhang, “LQG control of networked control systems with access constraints and delays,” *Int. J. Control*, vol. 81, no. 8, pp. 1266–1280, 2008.
- [S22] D. Maity, M. H. Mamduhi, S. Hirche, K. H. Johansson, and J. S. Baras, “Optimal LQG control under delay-dependent costly information,” *IEEE Contr. Syst. Lett.*, vol. 3, no. 1, pp. 102–107, 2019.
- [S23] S. Tatikonda and S. Mitter, “Control under communication constraints,” *IEEE Trans. Autom. Control*, vol. 49, no. 7, pp. 1056–1068, 2004.
- [S24] G. N. Nair, F. Fagnani, S. Zampieri, and R. J. Evans, “Feedback control under data rate constraints: An overview,” *Proc. IEEE*, vol. 95, no. 1, pp. 108–137, 2007.
- [S25] T. Tanaka, P. M. Esfahani, and S. K. Mitter, “LQG control with minimum directed information: Semidefinite programming approach,” *IEEE Trans. Autom. Control*, vol. 63, no. 1, pp. 37–52, 2018.
- [S26] A. Molin and S. Hirche, “On LQG joint optimal scheduling and control under communication constraints,” in *Proc. IEEE Conf. Decision and Control*, 2009, pp. 5832–5838.
- [S27] A. Molin and S. Hirche, “On the optimality of certainty equivalence for event-triggered control systems,” *IEEE Trans. Autom. Control*, vol. 58, no. 2, pp. 470–474, 2013.
- [S28] A. Molin and S. Hirche, “Price-based adaptive scheduling in multi-loop control systems with resource constraints,” *IEEE Trans. Autom. Control*, vol. 59, no. 12, pp. 3282–3295, 2014.
- [S29] C. Ramesh, H. Sandberg, and K. H. Johansson, “Design of state-based schedulers for a network of control loops,” *IEEE Trans. Autom. Control*, vol. 58, no. 8, pp. 1962–1975, 2013.
- [S30] Y. Xu and J. P. Hespanha, “Estimation under uncontrolled and controlled communications in networked control systems,” in *Proc. IEEE Conf. Decision and Control and European Control Conf.*, 2005, pp. 842–847.
- [S31] Y. Mo, R. Ambrosino, and B. Sinopoli, “Sensor selection strategies for state estimation in energy constrained wireless sensor networks,” *Automatica*, vol. 47, no. 7, pp. 1330–1338, 2011.
- [S32] L. Shi and H. Zhang, “Scheduling two Gauss–Markov systems: An optimal solution for remote state estimation under bandwidth constraint,” *IEEE Trans. Signal Process.*, vol. 60, no. 4, pp. 2038–2042, 2012.
- [S33] D. Han, J. Wu, H. Zhang, and L. Shi, “Optimal sensor scheduling for multiple linear dynamical systems,” *Automatica*, vol. 75, pp. 260–270, 2017.
- [S34] S. Wu, X. Ren, S. Dey, and L. Shi, “Optimal scheduling of multiple sensors with packet length constraint,” in *Proc. IFAC World Congr.*, 2017, pp. 14430–14435.
- [S35] D. E. Quevedo, A. Ahlén, and K. H. Johansson, “State estimation over sensor networks with correlated wireless fading channels,” *IEEE Trans. Autom. Control*, vol. 58, no. 3, pp. 581–593, 2013.
- [S36] A. S. Leong, D. E. Quevedo, A. Ahlén, and K. H. Johansson, “On network topology reconfiguration for remote state estimation,” *IEEE Trans. Autom. Control*, vol. 61, no. 12, pp. 3842–3856, 2016.
- [S37] T. Iwaki, Y. Wu, J. Wu, H. Sansberg, and K. H. Johansson, “Wireless sensor network scheduling for remote estimation under energy constraints,” in *Proc. IEEE Conf. Decision and Control*, 2017, pp. 3362–3367.
- [S38] A. S. Leong, S. Dey, G. N. Nair, and P. Sharma, “Power allocation for outage minimization in state estimation over fading channels,” *IEEE Trans. Signal Process.*, vol. 59, no. 7, pp. 3382–3397, 2011.
- [S39] K. Gatsis, A. Ribeiro, and G. J. Pappas, “Optimal power management in wireless control systems,” *IEEE Trans. Autom. Control*, vol. 59, no. 6, pp. 1495–1510, 2014.
- [S40] X. Ren, J. Wu, K. H. Johansson, G. Shi, and L. Shi, “Infinite horizon optimal transmission power control for remote state estimation over fading channels,” *IEEE Trans. Autom. Control*, vol. 63, no. 1, pp. 85–100, 2018.
- [S41] A. S. Leong and S. Dey, “Power allocation for error covariance minimization in Kalman filtering over packet dropping links,” in *Proc. IEEE Conf. Decision and Control*, 2012, pp. 3335–3340.
- [S42] D. E. Quevedo, A. Ahlén, A. S. Leong, and S. Dey, “On Kalman filtering over fading wireless channels with controlled transmission powers,” *Automatica*, vol. 48, no. 7, pp. 1306–1316, 2012.
- [S43] A. Nayyar, T. Başar, D. Teneketzis, and V. V. Veeravalli, “Optimal strategies for communication and remote estimation with an energy harvesting sensor,” *IEEE Trans. Autom. Control*, vol. 58, no. 9, pp. 2246–2260, 2013.
- [S44] M. Nourian, A. S. Leong, and S. Dey, “Optimal energy allocation for Kalman filtering over packet dropping links with imperfect acknowledgments and energy harvesting constraints,” *IEEE Trans. Autom. Control*, vol. 59, no. 8, pp. 2128–2143, 2014.
- [S45] S. Knorn, S. Dey, A. Ahlén, and D. E. Quevedo, “Optimal energy allocation in multi sensor estimation over wireless channels using energy harvesting and sharing,” *IEEE Trans. Autom. Control*, 2019. doi: 10.1109/TAC.2019.2896048.



**FIGURE 3** Iggesund's paper mill has two paper machines that are 300 m long and produce state-of-the-art cardboard. The photo is taken from the wet end of the cardboard machine 2. At the far right of the photo is the wire section, where the pulp comes out of the headboxes and is dewatered on the wire. At that point, the pulp contains more than 99% water. To the left is the drying unit, where the cardboard is dried by steam. (Source: Iggesund Paperboard; used with permission.)

(which require high quality). There is also a coating kitchen that delivers layers used to seal the paperboard to make it smooth and even (and hence, a good surface for printing, producing a high-quality product).

During the three-year project period, several live tests were conducted to evaluate wireless control in the industrial environment of the factory. These tests were implemented mainly in the coating kitchen, where there are two starch cookers. The starch production is an important ingredient when mixing and preparing the paperboard coating. The starch provides the finish and color of the paperboard, which is used for exclusive packaging of, for example, whiskey, perfumes, and chocolate. This process delivers coating to both paper machines, and the final quality of the paperboard depends on a constant supply of high-quality coating. The cookers are used to boil the starch, which is subsequently used in the manufacturing of the different coatings. Only one cooker was used to implement the wireless outbreak during the experiments,

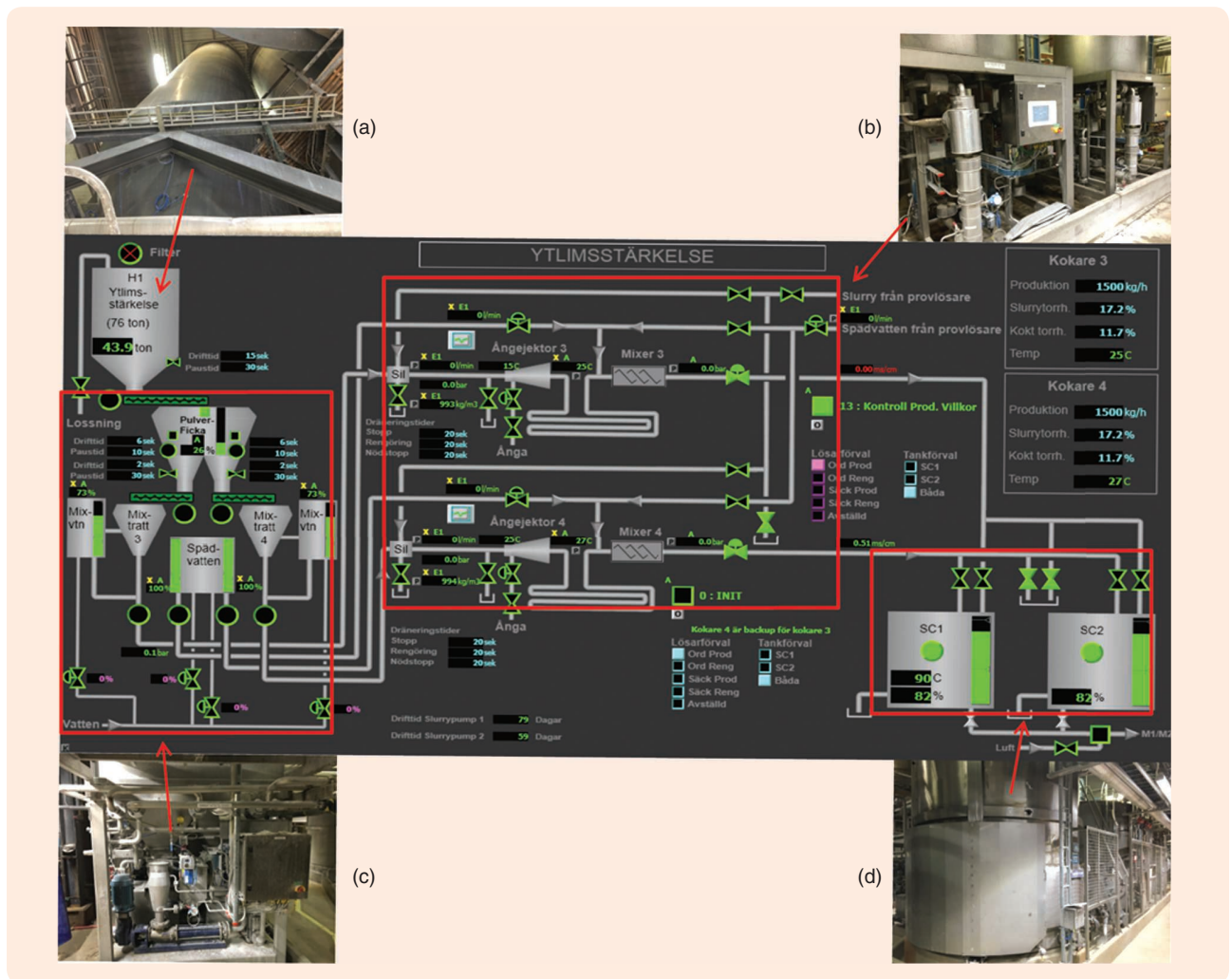


**FIGURE 4** The starch cooker process (illustrated by the operator panel in the middle) and photos of the real process equipment: (a) the starch powder buffer, (b) the starch boiler, (c) the mixing tank for starch powder and water, and (d) the storage tank for boiled starch. The red arrows relate the respective process equipment to the operator panel. (Source: Iggesund Paperboard; used with permission.)

while normal production continued on the other. Thus, the experiments did not disturb the production at the paperboard machines. The process in the cookers allows silo H1 [Figure 4(a)] to act as a buffer for the starch powder. From there, the powder is transported to a storage hopper with a level regulator to ensure the same degree of filling in the dosing screws. The dry powder mixes with water. Figure 4(c) shows this process, which is controlled by a concentration regulator. The mixture is then pumped into the steam ejector, where steam is added to boil the starch. The starch boiling process is controlled by a temperature regulator. After that, water is added again to obtain the correct dry content on the final product. A picture of the process where the starch is boiled is shown in Figure 4(b). The starch cooking is a batch process started and stopped automatically by the level in the storage tanks [Figure 4(d)].

### A WIRELESS CONTROL ARCHITECTURE FOR THE STARCH COOKER

Figure 5 shows a proposed wireless control architecture for the starch cooker process of the Iggesund Mill. The architecture consists of multiple wireless feedback loops involving sensors ( $S_j$ ) and actuators ( $A_j$ ). From the left in Figure 5, the cooker works as follows. Water from the mix water tank, the level of which is controlled by ( $S_1, A_1$ ), is mixed with starch powder distributed through the mix funnel. The properties of the starch-water mixture are governed by the concentration control loop ( $S_2, A_2$ ) and the coarse flow control loop ( $S_3, A_3$ ). The mixture is cooked using a steam injector, which is temperature controlled by ( $S_4, A_4$ ). The concentration of the starch solution is further diluted by the fine flow control loop ( $S_5, A_5$ ), after which a mixing and pressure control loop [governed by ( $S_6, A_6$ )] adds the final touch before the starch solution is sent to the storage tank. In our wireless setup, all control actions are calculated at the actuators in a distributed fashion, and the sensor and actuator information is sent to the GWs for further distribution to the operators.

### MODELING OF RADIO CHANNELS IN AN INDUSTRIAL ENVIRONMENT

When a wireless environment is static, the wireless link design is fairly straightforward, even if line-of-sight between the transmitting node and the receiving node cannot be obtained. It is then just a matter of selecting the appropriate number of sensor nodes and good locations and/or adjusting

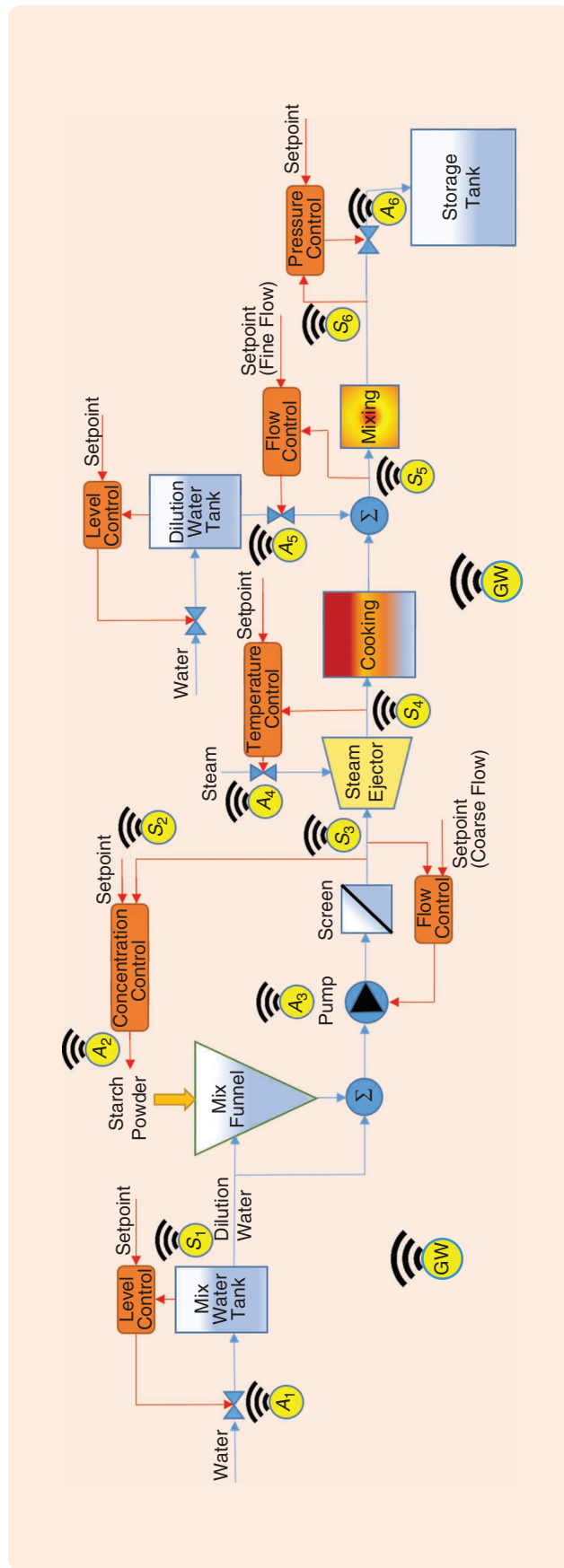


**FIGURE 5** A block diagram of the Iggesund Paperboard starch cooker, which is also illustrated in the operator's panel of Figure 4. The process starts with filling a water tank (depicted at top left), and that water is mixed with the starch in a mixing funnel. To remove lumps of starch, the mixture is pumped through a screen before steam is injected for cooking. To finely adjust the starch concentration after cooking, small amounts of dilution water may be added before storing the product in a storage tank (see the bottom-right corner). The architecture consists of multiple wireless feedback loops involving sensors ( $S_j$ ) and actuators ( $A_j$ ) to control each step of the process. GW: gateway.

the transmit power. However, even if an industrial environment looks static at a first glance, it is very seldom static over a long time horizon (several minutes and hours).

Typical indoor channels are well described by either log-normal (LN), Rayleigh, Rice, Nakagami- $m$  [Gamma (G) in the power domain], or Weibull distributions [1], [10]–[12]. The distribution that best fits the received data depends on the environment and the degree of motion around the communicating sensor nodes and the observation interval. For a comprehensive overview of radio-channel characteristics in indoor and industrial environments, see [11]–[13] and the

references therein. Furthermore, previous studies have observed that temporal channel variations in wireless sensor networks (WSNs) with stationary nodes (both the transmitting and receiving antennas are stationary) typically follow a Rician or Nakagami- $m$  distribution [1], [11], [14].

### Characterizing Channel Gain Variability

To obtain an accurate representation of the radio environment at the Iggesund paper mill, numerous point-to-point measurements were taken at different positions along the paper mill production line as well as in the starch cooker environment. In addition to these point-to-point measurements, numerous rig measurements were conducted. For the rig measurements, the location of the transmitter was fixed, whereas the receiver was moved in a controlled direction in space. The very common assumption in cellular communications that radio links are subject to Rayleigh fading (which typically arises when a receiver is moving through a standing wave pattern with multiple scatterers in the vicinity) was confirmed by numerous rig measurements from static environments in Iggesund [15]. However, extensive sensor-node-to-sensor-node measurement campaigns (conducted at Iggesund and two other process industries) confirmed that static channels are rare, particularly when observing the radio environment over several minutes and hours (see [15] and [16]).

The typical situation in industrial environments, like the one in Iggesund, is that wireless channel variability in node-to-node links is caused by objects moving in the vicinity of (or in between) the sensor nodes. Examples of such a channel gain variability for the paper mill and cooker environment are illustrated in Figure 6(a) and (b), respectively.

A closer look at Figure 6(a) reveals that the channel gain can vary by 20–30 dBm and remain in a higher or lower decibel region for several minutes or hours. In Figure 6(a), the link variability is caused by a crane (located in the ceiling of the building) moving finished, high-quality paper from the roll-up section to the floor and from one location on the floor to another (where it is temporarily stored for later cutting and long-term storage). In this case, the intermediate storage of the paper rolls shadowed the radio link between the two nodes, causing a significant change in the channel gain [see Figure 7(a)]. In the time interval 4.5–8.5 h in Figure 6(a), the intermediate storage on the floor next to the roll-up section was cleared, and the channel gain increased for a period of several hours. A similar channel gain variability was observed at several other locations at the paper mill. However, at the starch cooker location [see Figure 7(b)], the channel gain variability was primarily caused by people moving in the narrow aisle close to the sensor node locations [see Figure 6(b)]. Here, the variability was in the range of 10–20 dBm. This indicates that careful channel modeling is required should energy-efficient and low-latency communications be attained, constituting a prerequisite for low-latency controller design.

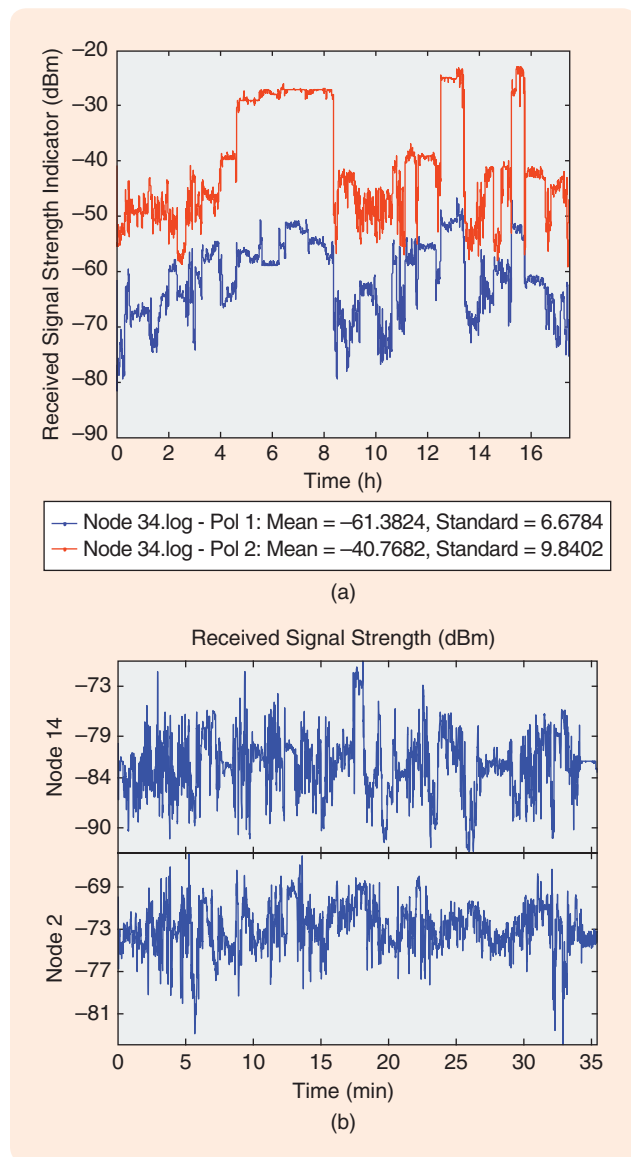


**FIGURE 6** The channel gain variability between two sensor nodes located next to the paper machine finish line at Iggesund. The crane in the ceiling moving around the paper rolls causes the gain variability. (a) The vertical polarization (red), horizontal polarization (blue), and channel gain variability realizations between two pairs of sensor nodes in the starch cooker section (b). The variability is primarily caused by people moving in the environment of the sensor nodes.

## Parameter Estimation

Considering the variability of several links, a maximum likelihood estimation of the model parameters reveals that neither Rayleigh, Rice, nor LN distributions are solely adequate for describing the fading characteristics in a typical paper mill environment (see Figure 8). It is clear that the Nakagami-LN [Gamma-LN (GLN) in the power domain] compound distribution gives the best fit to the link measurement data acquired from the extensive measurement campaign conducted at the paper mill. In Figure 8, (a) depicts the estimated and empirical cumulative power-level distribution in decibels, whereas (b) illustrates the theoretical and empirical average bit error rates

(BERs) for different distributions. Selecting the wrong fading distribution will have a detrimental effect on both energy expenditure and BERs. In Figure 8, a one-component compound distribution was considered. However, when performing a more in-depth identification based on the Iggesund measurement data over different time horizons, two fading components (see "Radio Model Selection") are frequently required, as illustrated in Table 1. Measurement campaigns conducted at other industrial sites show that three components might even be required in some cases. From Table 1, observe that for 1-h segments, one component suffices in 59% of the cases. In those one-component cases, a GLN channel

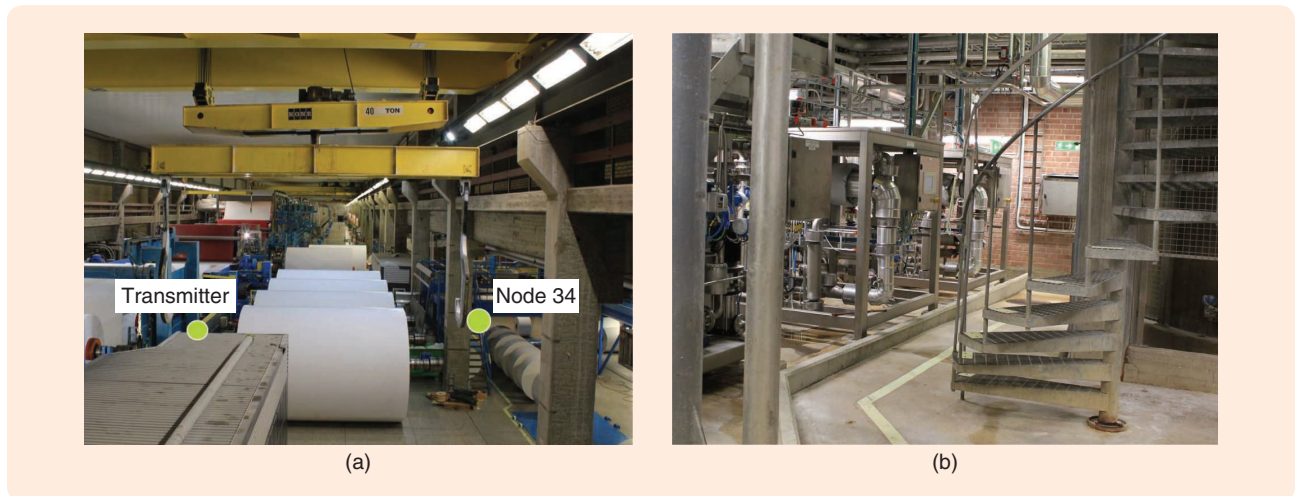


**FIGURE 7** The Iggesund Paperboard paper mill. (a) The channel measurement between two nodes located on opposite sides of the aisle next to the paper mill finish line in Iggesund. The green dots indicate the approximate positions of the sensor nodes. A typical channel gain variability is depicted in Figure 6(a). (b) An aisle in the cooker environment where wireless sensor nodes were deployed. Typical channel gain variabilities between pairs of nodes are depicted in Figure 6(b). (Source: Iggesund Paperboard; used with permission.)

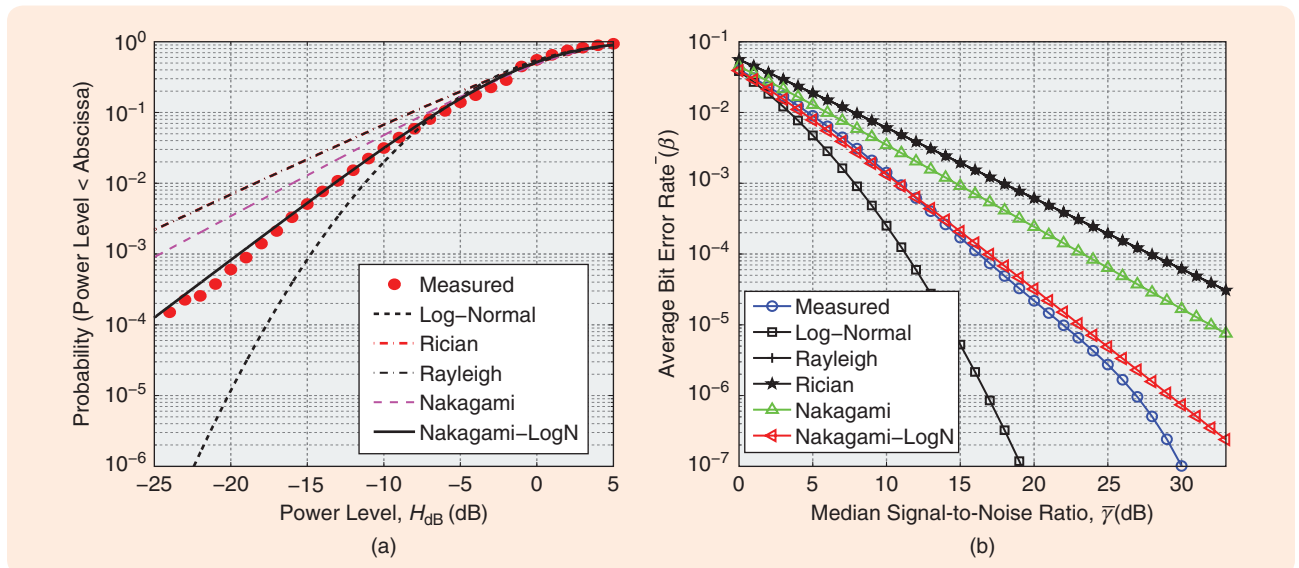


**FIGURE 8** The theoretical and empirical evaluations taken over all wireless link data acquired during a measurement campaign at Iggesund Mill, Sweden, over 17 h. (a) The estimated and empirical cumulative power-level distributions (in decibels) based on all measured links over 17 h. (b) The theoretical and empirical average bit error rate as a function of the median signal-to-noise ratio based on all measured links over 17 h [15].

## Radio Model Selection

Radio links similar to those depicted in Figure 6 can be modeled as a mixture probability density function (pdf) with  $M$  components

$$p(y|\varphi) = \sum_{i=1}^M P_i p(y|\theta_i), \quad (S1)$$

where  $y$  is the underlying continuous variable representing power,  $P_1, \dots, P_M$  are mixture probabilities satisfying  $\sum_i P_i = 1$ ,  $p(y|\theta_i)$  is the pdf of the  $i$ th mixture component described by the parameter vector  $\theta_i$ , and  $\varphi = \{\theta_1, \dots, \theta_M, P_1, \dots, P_M\}$ .

The corresponding discrete distribution for quantized data is obtained by integration over the user-selected bin intervals  $I_k$ ,  $\forall k$ , that is,

$$P(k|\varphi) \triangleq Pr(y \in I_k|\varphi) = \int_{y \in I_k} p(y|\varphi) dy; \quad \forall k. \quad (S2)$$

As explained in the following (see also Figure 8), an individual mixture component  $p(y|\theta_i)$  is preferably modeled as either purely Gamma (G), log-normal (LN), or GLN distributed. The G distribution in the power domain is given by

$$p_G(y) = \frac{m^m \exp\left(m \frac{y-\bar{y}}{\mu}\right) \exp\left(-m \exp\left(\frac{y-\bar{y}}{\mu}\right)\right)}{\mu \Gamma(m)}, \quad (S3)$$

where  $\bar{y}$  is the mean,  $\mu$  is a constant, and  $m$  is the Nakagami- $m$  parameter. Hence, the pure G component can be parameterized by  $\theta_i = (\bar{y}_i, m_i)$ .

The compound GLN fading model arises for a power gain that is the product of two independent factors, where one is G distributed and one is LN distributed. Expressed in decibels, the LN distribution is

$$p_{LN}(y) = \frac{1}{(2\pi)^{1/2} \sigma} \exp\left(-\frac{y^2}{2\sigma^2}\right), \quad (S4)$$

where  $\sigma$  is the standard deviation and where, without loss of generality, the mean must be set to zero. Expressed in  $y$ , the previously mentioned product becomes a sum of independent variables, and the resulting pdf for this sum,  $p_{GLN}(y)$ , is given by the convolution  $p_{GLN}(y) = p_G(y) * p_{LN}(y)$ . The GLN component is thus parameterized by the tuple  $\theta_i = (\bar{y}_i, m_i, \sigma_i)$ .

model best fits the data in 39% of the cases, whereas in 20% of the cases, a G channel model is sufficient. In 34% of the total cases, a two-component compound model consisting of either G or GLN combinations is the best choice.

The situation is similar for 4-h segments. However, in this case, a two-component compound model is somewhat less frequent. For the 16-h segments, in only 15% of the cases was a two-component compound model appropriate. Therefore, in most cases, a one-component GLN model is a good description of the link variability at the Iggesund site. In other cases (for the Sandviken rolling mill measurement

campaign), a two-component model was the most appropriate choice for the 16-h segments. These findings suggest that, before a wireless control network is to be deployed at a new industrial site, a measurement campaign should be conducted to determine the required complexity of the fading distributions. Both better BERs and energy expenditure figures can then be obtained.

## Modeling Joint Behavior of Radio Channels in Industrial Environments

In this section, the analysis of the radio-channel measurements from the previous section is extended to study the joint behavior of radio links. Specifically, by partitioning the link measurements into volatile and quiescent periods using hidden Markov models (HMM), we identify the links that are likely to simultaneously experience severe fading. The study is motivated by emerging routing protocols for WSNs where multipath diversity was considered a key for achieving timely data transfer [17].

These protocols transmit multiple copies of each data packet over parallel paths, and this technique is most effective if transmission failures over the paths are uncorrelated. For instance, if a single event affects the quality of several paths, then there is little gain from the multipath diversity. When a sensor node has multiple neighbors, the gain from the multipath diversity is increased if the selection process uses information on correlations in link quality among its neighbors. This section outlines an algorithm for detecting such correlations. We also demonstrate the performance of the algorithm on measurements of channel gains obtained

**TABLE 1** The obtained number of mixture components (Comp) percentage after maximum likelihood-optimization over 1-, 4-, and 16-h time segments acquired at Iggesund Paperboard in Sweden. The models were identified and validated based on received signal strength (RSS) power measurements (see “Radio Model Selection”): Gamma (G) and/or gamma-log-normal (GLN) compound models. (L) is lost packets, where RSS data could not be retrieved. The total number of time segments: 92 (46) for 1 h and 4 h (16 h).

Segment (h)	1 Comp		2 Comp			L
	G	GLN	G-G	G-GLN	GLN-GLN	
1	20	39	13	14	7	7
4	23	36	11	10	6	14
16	30	42	7	4	4	13

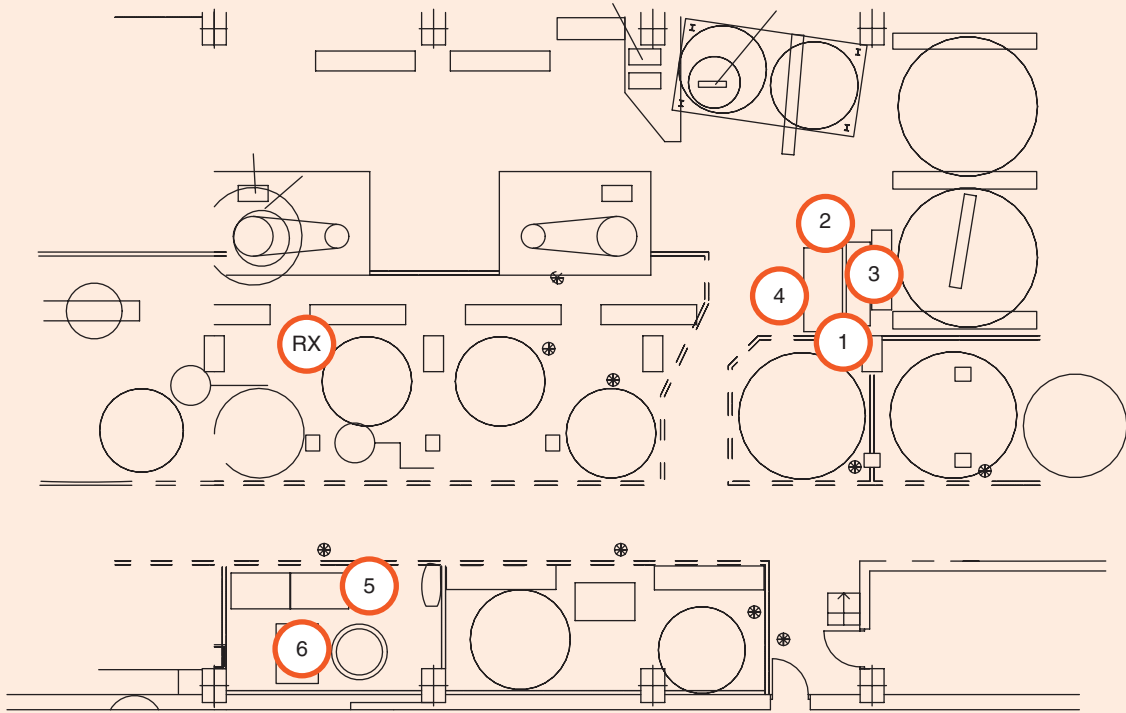


**FIGURE 9** An overview of the deployment area at the paper mill in Iggesund. The circles indicate the positions of the wireless sensor nodes that were deployed in close proximity to machines to mimic a realistic wireless control scenario.

from a network of nodes deployed in the vicinity of the starch cooker. The results show that it is common for some links to undergo joint changes in link quality, and we describe how this information could be incorporated into the design of multipath routing protocols.

### Measurements

For the purpose of the analysis in this section, we focus on measurements obtained from seven wireless sensor nodes. These were deployed in the vicinity of the starch cooker. Figure 9 illustrates a map of the deployment area, which included heavy machines and a large amount of metal objects.

In Figure 9, a scenario is illustrated where the node marked RX is a sensor node that is listening to transmissions from six of its neighbors that are all closer to the intended GW (not depicted in the figure). The objective of the RX node is to select a subset of these neighbors as relaying nodes. As will be described in more detail in the next section, the subset should be chosen so that the gain from the multipath diversity is increased.

The transmissions were performed in a round-robin fashion, where each of the nodes labeled 1–6 sent a packet to the RX node, which recorded the received signal strength (RSS) of the incoming transmissions. Each node sent a packet every 0.125 s, and measurements were conducted for 3 h. A short segment of the resulting time series is illustrated in Figure 10.

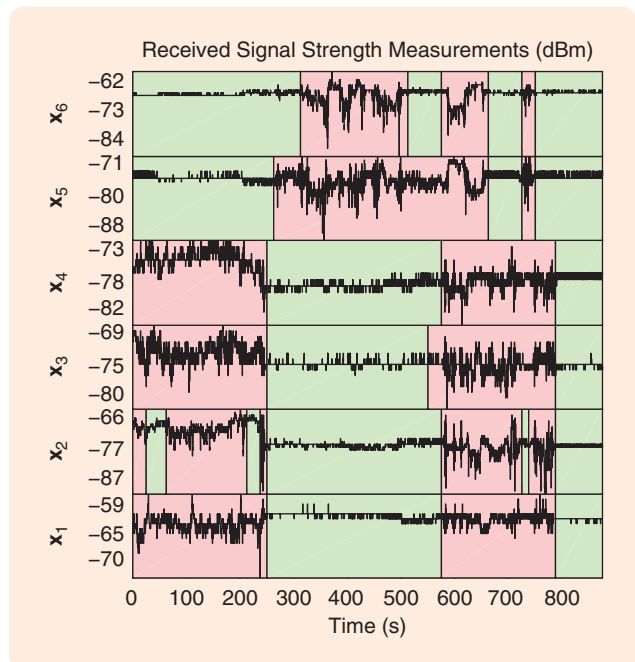


**FIGURE 10** A time series of recorded received signal strengths for the network in Figure 9. The green and pink fields mark the estimated periods of quiescent and volatile fading, where  $\hat{z}_{i,t} = 0$  and  $\hat{z}_{i,t} = 1$ , respectively. Since nodes  $x_1$ – $x_4$  were positioned relatively close to each other, they often were in the same fading state. As expected, nodes  $x_5$  and  $x_6$  exhibited similar behavior.

As described in the previous section, the fading distribution of each link switched abruptly between volatile and more quiescent periods, where the channel gain could vary on the order of 20 dB in the former case. Moreover, initial studies of the measurements showed that, for each link, the volatile periods had a roughly similar spectrum. Hence, to detect changes in volatility of the monitored links, we propose a two-state HMM, where each state generates observations from an autoregressive (AR) process. For future reference, let  $\hat{z}_{l,t}$  denote the state of link  $l$  at time  $t$ , where  $\hat{z}_{l,t} = 1$  indicates the volatile fading state and  $\hat{z}_{l,t} = 0$  the quiescent fading state. In [18], Rabiner outlined an algorithm for inference of such models. The most important steps are summarized in “Data Generation Model.” Finally, the inferred state sequence, which partitions each link into periods of volatile and quiescent behavior, will be used to identify links that are likely to experience severe fading simultaneously.

## Results

Movement in the vicinity of the nodes mostly consisted of personnel walking along the paths that are marked by double dashed lines in Figure 9. Since the nodes were positioned in

two clusters (where, for future reference, cluster 1 denotes nodes 1–4 and cluster 2 denotes nodes 5–6), passing personnel induced time-varying shadow fading that often affected all of the links in a cluster. However, due to the spatial separation between the clusters, it was unlikely that both of them were shadowed simultaneously.

In Figure 10, the background color indicates the estimated state sequence  $\hat{z}_l$  from the HMMs. As expected, there is a tendency for the nodes in cluster 1 to have overlapping volatile regions. The same tendency can be observed for cluster 2. However, the volatile regions between nodes from different clusters show more sporadic overlap.

Table 2 lists the empirical probabilities,  $o_{ij}$ , that  $\mathbf{x}_j$  is in the volatile state given that  $\mathbf{x}_i$  is in the volatile state, which can be computed as

$$o_{ij} = \frac{\sum_{t=1}^T \hat{z}_{i,t} \hat{z}_{j,t}}{\sum_{t=1}^T \hat{z}_{i,t}}. \quad (1)$$

The blue and red fields highlight the sparsity of the table, which indicates that, for instance, if  $\mathbf{x}_1$  is in the volatile

### Data Generation Model

Let  $\mathbf{x}_l = [x_{l,1}, \dots, x_{l,T}]$  denote  $T$  scalar received signal strength (RSS) measurements from the  $l$ th link. The observations in  $\mathbf{x}_l$  are assumed to be generated by a two-state hidden Markov models (HMM), where  $z_{l,t} \in [0, 1]$  denotes the state of the model associated with the  $l$ th time series at time  $t$ . As described in more detail in the following,  $z_{l,t}$  parameterizes the generative distribution of  $x_{l,t}$ . The state sequence  $\mathbf{z}_l = [z_{l,1}, \dots, z_{l,T}]$  is generated by a Markov model with transition probabilities,  $Q_l = \{q_{l,i,j} : i, j \in [1], [2]\}$ , where  $q_{l,i,j}$  denotes the probability

$$q_{l,i,j} = P(z_{l,t+1} = j | z_{l,t} = i). \quad (S5)$$

The initial state distribution is denoted as  $\boldsymbol{\pi}_l = \{\pi_{l,i} : i \in [1], [2]\}$ , where

$$\pi_{l,i} = P(z_{l,1} = i). \quad (S6)$$

Each state generates observations from an autoregressive process, such that

$$x_{l,t} = \mathbf{x}_{l,t-1:t-v} \mathbf{a}'_{l,z,t} + e_{l,t}, \quad (S7)$$

where  $\mathbf{a}_{l,z} = [a_{l,z,1}, \dots, a_{l,z,v}]$  are the AR coefficients for state  $z$ ,  $v$  is the order of the process, and  $e_{l,t}$  is independent, zero-mean Gaussian noise with variance  $\sigma_{l,z}^2$ .

The states were labeled so that state  $z_{l,t} = 1$  corresponds to the more volatile fading state, for example,

$\sigma_{l,1}^2 > \sigma_{l,0}^2$ . In addition  $v = 2$  is fixed, which results in a satisfactory segmentation performance for all time series. Let  $\Lambda_l = \{Q_l, \boldsymbol{\pi}_l, \mathbf{a}_l, \boldsymbol{\sigma}_l\}$  denote the collection of model parameters, where  $\mathbf{a}_l = \{\mathbf{a}_{l,z} : z \in [1], [2]\}$  and  $\boldsymbol{\sigma}_l = \{\sigma_{l,z}^2 : z \in [1], [2]\}$ .

### ESTIMATION OF MODEL PARAMETERS

In [18], Rabiner outlined an iterative algorithm for computing the maximum likelihood estimate,  $\hat{\Lambda}_l$ , of the model parameters,

$$\hat{\Lambda}_l = \underset{\Lambda_l}{\operatorname{argmax}} P(\mathbf{x}_l | \Lambda_l). \quad (S8)$$

The interested reader is referred to the original work for details on the algorithm.

Since the inference objective is to use the HMM to detect changes in volatility, the RSS measurements were preprocessed with a bandpass filter with cutoff frequencies at  $[1/2, 2]$  Hz. This eliminated slow-varying trends and measurement noise from  $\mathbf{x}_l$  prior to estimation of  $\hat{\Lambda}_l$ .

### INFERENCE OF THE STATE SEQUENCE

Conditioned on  $\hat{\Lambda}_l$ , the most likely state sequence,  $\hat{\mathbf{z}}_l = [\hat{z}_{l,1}, \dots, \hat{z}_{l,T}]$ , is obtained by maximizing

$$\hat{\mathbf{z}}_l = \underset{\mathbf{z}_l}{\operatorname{argmax}} P(\mathbf{x}_l, \mathbf{z}_l | \hat{\Lambda}_l), \quad (S9)$$

and the solution can be computed using the Viterbi algorithm in [18].

state, then it is likely that  $x_2$ ,  $x_3$ , and  $x_4$  are also in the volatile state. However, it is less likely that  $x_5$  or  $x_6$  is in the volatile state.

In summary, by using HMMs, a sensor node can identify correlations in link quality among its neighbors. This information can potentially be useful in a scenario where the node wants to transmit data to a sink node using a subset of these neighbors as relaying nodes. In this case, the robust choice (in the sense that the selected paths drop packets independently) is to send the packet to the neighbors that exhibit no or weak correlation in link quality.

### ENERGY HARVESTING IN WIRELESS NETWORKS

Employing many additional sensors in a large plant can have several significant advantages, including enabling more complex signal processing and control algorithms due to more information being available. Using wireless sensors and appropriate routing protocols (as described previously) already simplifies this process by avoiding wires for information flow. Flexibility, when adding wireless sensors to the plant, can further be enhanced if the sensors do not have to be connected to the electricity grid but, instead, are powered using energy harvesting. For instance, at the starch cooker at the Iggesund Mill, several energy sources (hot pipes or tanks, rotating or vibrating parts, or lighting) can be used to extract energy to power wireless sensors.

To study the energy-harvesting capabilities at Iggesund Mill, several wireless energy-harvesting sensors were employed. Some sensors [see Figure 11(a)] were equipped with small solar cells to harvest energy from the lighting. Since some mixing tanks and pipes get very hot, the resulting large temperature gradients can be used to harvest energies using Peltier elements, as shown in Figure 11(b). The harvested energy was stored in a local rechargeable battery to be used for data transmission immediately or at a later stage.

**TABLE 2** The empirical probabilities computed using (1), where  $o_{i,j}$  is the element in the  $i$ th row and the  $j$ th column. The background colors highlight the block diagonal structure of the matrix, which implies that the nodes belong to two distinct groups, where the nodes within the same group often were in the same fading state.

%	$x_1$	$x_2$	$x_3$	$x_4$	$x_5$	$x_6$
$x_1$	.	0.74	0.90	0.79	0.17	0.14
$x_2$	0.96	.	0.96	0.95	0.16	0.14
$x_3$	0.67	0.55	.	0.75	0.16	0.14
$x_4$	0.75	0.68	0.95	.	0.15	0.12
$x_5$	0.23	0.17	0.29	0.22	.	0.7
$x_6$	0.28	0.21	0.3	0.25	0.99	.

A simple algorithm was then used to control the sensors. Measurements should be submitted every 1–3 s if sufficient energy is available in the sensor’s battery or, otherwise, as soon as enough energy is available again. Figure 12 shows the time between consecutive packets received from a wireless sensor located close to node 4 in Figure 9 for a measurement campaign over several hours. Here, the harvested energy varies periodically since the pipe delivers a product of a reoccurring batch process of slightly more than 1 h in length. Since the energy is harvested from a hot pipe, the amount harvested significantly

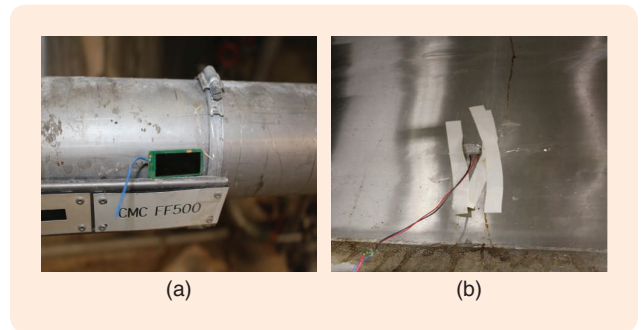


**FIGURE 11** Images obtained from the starch cooking process. (a) A pipe in the starch cooking environment and (b) a storage tank for the boiled starch. (Source: Iggesund Paperboard; used with permission.)

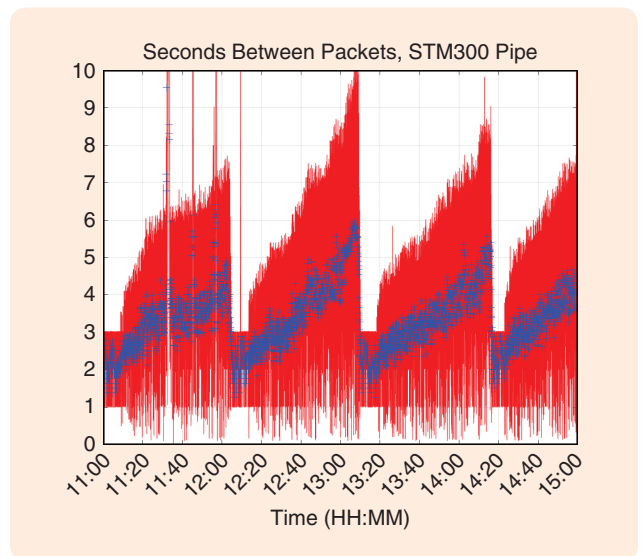


**FIGURE 12** The time between consecutive packets received from a wireless sensor at node 4 powered by a Peltier element attached to a hot pipe: raw data (red) and filtered (blue). It is clearly visible that the time between two consecutive packets changes periodically because the harvested energy used to send the packets also changes periodically. The pipe at which the Peltier element was located transports hot liquids to a batch process. This takes a few minutes, and the pipe gets very hot. Afterward, the temperature decreases slowly, so that the harvested energy also gradually decreases, and the time between the packets increases. The batch process is then repeated roughly every hour so that the patterns repeat periodically.

depends on the temperature of the pipe, which varies periodically due to the batch process. Thus, when the pipe cools down after the necessary amount of hot liquid has been delivered for the current batch, less energy can be harvested, and the time between sent packets increases, as observed in Figure 12. Large time gaps between consecutive packets, and long periods of time where no packets can be sent due to a lack of harvested energy, are highly undesirable in practical settings. One method to improve this situation is to derive better algorithms to allocate the available harvested energy. For the energy-harvesting scenario illustrated in Figure 12, information about or a model of the underlying batch process should be used to predict and plan for the available harvested energy over time so that the maximal time between consecutive packets is minimized.

To model the available energy over time, first denote the harvested energy at sensor  $m$  and time slot  $k$  by  $H_m(k)$ . Several methods exist to model the harvested energy (Markov chains) motivated by empirical measurements reported in [19]. For the underlying harvesting process in Figure 12, additional information, including the temperature of the liquid in the pipe, can be used to derive more accurate models. The energy harvested at time slot  $k$  is stored in the battery, and it can be used for different tasks (data transmission) in the  $k + 1$ th time slot. Hence, the dynamics of the battery level of sensor  $m$  at time  $k + 1$  can be described by  $B_m(k)$ , evolving according to

$$B_m(k + 1) = \min\{B_m(k) + H_m(k) - E_m(k); \hat{B}_m\}, \quad (2)$$

where  $E_m(k)$  denotes the energy used by sensor  $m$  at time  $k$  and  $\hat{B}_m$  denotes the battery capacity.

This battery model, together with a model for the harvesting process, can then be used to derive suitable energy allocation policies. If the harvesting sensor should transmit data over a fading channel, then an optimal energy allocation policy can be derived that chooses suitable transmission energies based on the battery level and the channel gain to maximize a desired quantity of interest.

## EVENT-BASED CONTROL

In event-based networked control systems, sensors transmit only when certain conditions are satisfied. Such systems have been quite widely studied over the last few decades, motivated by their lower requirements on communication compared to conventional periodic control (see ‘‘Advances in Event-Based Control’’). This section discusses the event-based control of the starch cooker process with wireless sensors, as illustrated in Figure 5. Specifically, we describe how event-based feedback and feedforward control are implemented for that process.

The focus of the discussion is on one specific control loop of the starch cooker, that is, the fine water flow control.

The fine water flow is controlled by sensor  $S_5$  and actuator  $A_5$  in Figure 5 to obtain the desired final starch paste solution. The concentration is possibly disturbed by the change of the steam flow into the steam ejector or the change of the starch concentration after the screen. Since such a disturbance only slowly affects the final product, it is difficult to mitigate the influence effectively by feedback control. Feedforward compensation adjusts the fine water flow rate as soon as the disturbance is detected. To do this, the steam flow and the opening of the steam valve are monitored by sensor  $S_4$  and actuator signal  $A_4$ , respectively. Since disturbances act sporadically, it is reasonable to use event-based compensation (in other words, to let  $S_4$  and  $A_4$  transmit their sensor and actuator values only when each value changes more than a certain threshold). The merits of such an event-based feedforward compensation scheme and the event-based feedback control are illustrated in this section. To mimic a control loop in the starch cooker, a continuous-time linear system is given by

$$\dot{x}_p(t) = Ax_p(t) + Bu(t) + \tilde{B}w(t), \quad (3)$$

$$y(t) = Cx_p(t), \quad (4)$$

where  $x_p$  is the plant state,  $y$  the plant sensor output,  $w$  the disturbance, and  $u$  the control input to the plant. The disturbance  $w$  affects the plant through the disturbance dynamics

$$\dot{w}(t) = A_d w(t) + B_d d(t), \quad (5)$$

where  $d$  is the external disturbance that can be measured by the disturbance sensor  $y_d(t) = C_d d(t)$ . For this system, a proportional-integral (PI) controller with discrete sampling is implemented as

$$\begin{aligned} \dot{x}_c(t) &= y(t_k) - r(t) \\ u(t) &= K_p(y(t_k) - r(t)) + K_i x_c(t) + K_f y_d(t_\ell), \end{aligned}$$

where  $x_c$  is the integrator state,  $r$  the reference (setpoint) signal,  $t_k$  the time of sample  $k$  of the event generator of the plant sensor, and  $t_\ell$  the time of sample  $\ell$  of the disturbance sensor.  $K_p$  and  $K_i$  are appropriately tuned proportional and integral gains, respectively. The feedforward gain is denoted  $K_f$ . The block diagram of the event-based control system is depicted in Figure 13.

Consider the event-based feedforward control, corresponding to the event generator in the feedback loop of Figure 13, to be periodic. A disturbance event is generated at the sensor when the condition  $|y_d(t) - y_d(t_i)| \geq \bar{e}_d$  is satisfied, where  $t_i$  is the last measurement instance and  $\bar{e}_d$  is a prespecified event threshold.

Figure 14 shows three simulations of disturbance responses for a first-order system with and without feedforward control and with PI feedback control in all three cases. Note that periodic samplings of the feedback control loop

## Advances in Event-Based Control

Event-based sampling for the classical feedback control loop has been studied, often as a means to reduce communications among the system components without sacrificing performance (see [S46]–[S48] and the references therein).

Optimal estimation and linear-quadratic-Gaussian (LQG) control with event-based sampling strategies are discussed by many researchers. The authors of [S49] offer a deterministic event-based scheduler using feedback from the estimator. A stochastic schedule is proposed in [S50]. With a similar setup, a scheduling framework where the transmissions are invoked by the estimation error covariance is proposed in [S51]. In [S52], packet dropouts are considered for covariance-based state estimation. These works are then extended to the LQG control problems in [S53]. In [S54], a time-division, multiple access-like, time-triggered schedule and a carrier sense, multiple access-like, event-triggered schedule with random or dynamic scheduler are analyzed. Multihop networks are explicitly considered in some studies. The LQG control with event-based sampling is investigated in [S27], where an optimal design of the controller and the event-triggering law is obtained. The tradeoff between LQG control performance and communication load for stochastic event-based control is discussed in [S55]. LQG control where the event-based communication is performed over Wi-Fi is considered in [S56].

To implement event-based control strategies into industrial control loops, event-based proportional-integral-derivative (PID) control has been considered, for example, in [21], [22], [27], and [S57]–[S60]. The works include both academic and industrial perspectives. As presented in [21], event-based PID control can significantly reduce the communication effort with only a slight or no degradation in control performance, which motivated the process industry to use event-based PID control [28]. In [24] and [25], event-based PID control is evaluated at an industrial paper mill plant in Iggesund. Some practical problems when introducing event-based PI control are discussed in [27], [26], and [S59]. In [27], it is shown that event-based sampling may result in a sticking effect or stationary large oscillations. To overcome these problems, [27] proposes PIDPLUS [S61]–[S63]. The asymptotic stability conditions are derived with a relative threshold policy in [S59]. Furthermore, [26], [S60], [S64], and [S65] focus on actuator saturation for event-based control. The stability region is influenced by the use of event-based control. In [26], it is shown that an antiwindup technique can significantly improve the performance for event-based control systems saturation. In [S65], an event-based antiwindup scheme is introduced. In [S60], a zero-order hold between the controller and the actuator is considered, and asymptotic stability conditions subject to actuator saturation are derived. Other PID controller design problems are

considered in [S58] and [S59]. In [S58], an LQ control design problem with event-based sampling is introduced. PI control synthesis with a relative threshold strategy is proposed in [S59].

## REFERENCES

- [S46] W. M. H. Heemels, J. Sandee, and P. van den Bosch, "Analysis of event-driven controllers for linear systems," *Int. J. Control*, vol. 81, no. 4, pp. 571–590, 2008.
- [S47] J. Lunze and D. Lehmann, "A state-feedback approach to event-based control," *Automatica*, vol. 46, no. 1, pp. 211–215, 2010.
- [S48] W. M. H. Heemels, K. H. Johansson, and P. Tabuada, "An introduction to event-triggered and self-triggered control," in *Proc. IEEE Conf. Decision and Control*, 2012, pp. 3270–3285.
- [S49] J. Wu, Q.-S. Jia, K. H. Johansson, and L. Shi, "Event-based sensor data scheduling: Trade-off between communication rate and estimation quality," *IEEE Trans. Autom. Control*, vol. 58, no. 4, pp. 1041–1046, 2013.
- [S50] D. Han, Y. Mo, J. Wu, S. Weerakkody, B. Sinopoli, and L. Shi, "Stochastic event-triggered sensor schedule for remote state estimation," *IEEE Trans. Autom. Control*, vol. 60, no. 10, pp. 2661–2675, 2015.
- [S51] S. Trimpe and R. D'Andrea, "Event-based state estimation with variance-based triggering," *IEEE Trans. Autom. Control*, vol. 59, no. 12, pp. 3266–3281, 2014.
- [S52] A. S. Leong, S. Dey, and D. E. Quevedo, "Sensor scheduling in variance based event triggered estimation with packet drops," *IEEE Trans. Autom. Control*, vol. 62, no. 4, pp. 1880–1895, 2017.
- [S53] A. S. Leong, D. E. Quevedo, T. Tanaka, S. Dey, and A. Ahlén, "Event-based transmission scheduling and LQG control over a packet dropping link," in *Proc. IFAC World Congr.*, 2017, pp. 8945–8950.
- [S54] M. Xia, V. Gupta, and P. J. Antsaklis, "Networked state estimation over a shared communication medium," *IEEE Trans. Autom. Control*, vol. 62, no. 4, pp. 1729–1741, 2017.
- [S55] B. Demirel, A. S. Leong, V. Gupta, and D. E. Quevedo, "Trade-offs in stochastic event-triggered control," *IEEE Trans. Autom. Control*, vol. 62, no. 6, pp. 2973–2980, 2018.
- [S56] M. Pezzutto, F. Tramarin, S. Dey, and L. Schenato, "SNR-triggered communication rate for LQG control over Wi-Fi," in *IEEE Conf. Decision and Control*, 2018, pp. 1725–1730.
- [S57] S. Reimann, W. Wu, and S. Liu, "PI control and scheduling design for embedded control systems," in *Proc. IFAC World Congr.*, 2014, pp. 11,111–11,116.
- [S58] J. G. Silva Jr., W. F. Lages da, and D. Sbarbaro, "Event-triggered PI control design," in *Proc. IFAC World Congr.*, 2014, pp. 6947–6952.
- [S59] S. Reimann, D. H. Van, S. Al-Areqi, and S. Liu, "Stability analysis and PI control synthesis under event-triggered communication," in *Proc. European Control Conf.*, 2015, pp. 2174–2179.
- [S60] L. Moreira, L. Groff, J. G. da Silva, and S. Tarbouriech, "Event-triggered PI control for continuous plants with input saturation," in *Proc. American Control Conf.*, 2016, pp. 4251–4256.
- [S61] J. Song, A. K. Mok, D. Chen, M. Nixon, T. Blevins, and W. Wojsznis, "Improving PID control with unreliable communications," in *Proc. ISA EXPO Technical Conf.*, 2006, pp. 17–19.
- [S62] O. Kaltiokallio, L. M. Eriksson, and M. Bocca, "On the performance of the PIDPLUS controller in wireless control systems," in *Proc. Mediterranean Conf. Control and Automation*, 2010, pp. 707–714.
- [S63] T. Blevins, M. Nixon, and W. Wojsznis, "PID control using wireless measurements," in *Proc. American Control Conf.*, 2014, pp. 790–795.
- [S64] D. Lehmann, G. A. Kiener, and K. H. Johansson, "Event-triggered PI control: Saturating actuators and anti-windup compensation," in *Proc. IEEE Conf. Decision and Control*, 2012, pp. 6566–6571.
- [S65] D. Lehmann and K. H. Johansson, "Event-triggered PI control subject to actuator saturation," in *Proc. IFAC Conf. Advances in PID Control*, 2012, pp. 430–435.

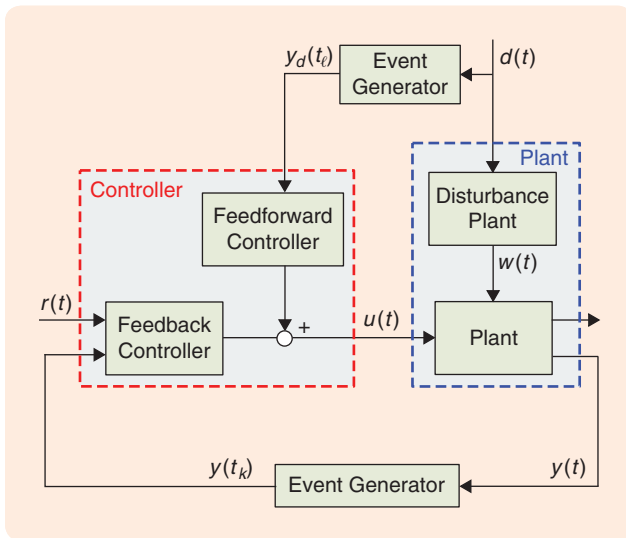


**FIGURE 13** A block diagram of the event-based feedback and feedforward control. The red box indicates the controller. The feedforward controller adjusts the control signal from the feedback controller based on the information from the disturbance sensor. The blue box indicates the plant, which consists of the disturbance plant and main plant. Event generators are introduced at the plant and disturbance sensors. Transmission events are generated if the sensor measurements change significantly.

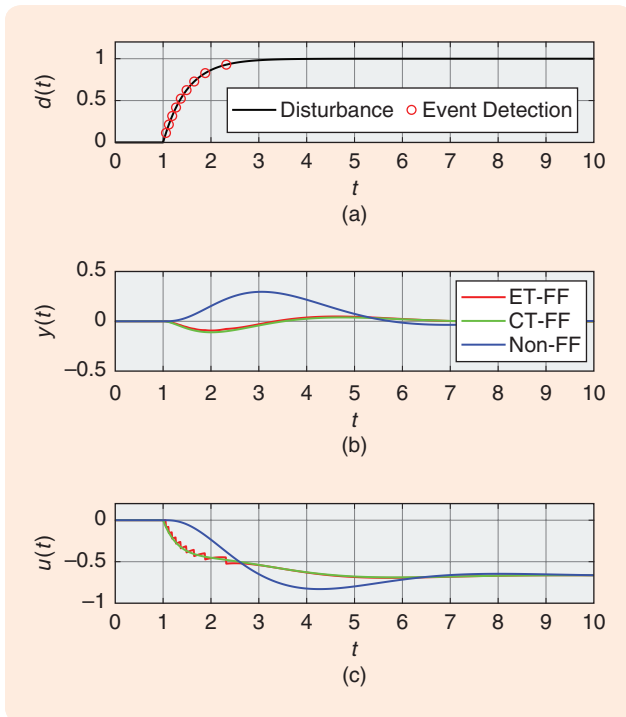


**FIGURE 14** Simulations of disturbance responses. (a) Disturbance and event-generation times. (b) The outputs of three cases: 1) event-based feedforward control (ET-FF) in red, 2) continuous-time feedforward control (CT-FF) in green, and 3) no feedforward control (non-FF) in blue. (c) Inputs of the same three cases. The simulations show that the ET-FF control performs as well as the CT-FF control with only nine transmissions of the disturbance measurements. See [20] for more details.

are considered in all cases. In Figure 14, (a) shows the disturbance, (b) shows the plant state, and (c) shows the PI control signal. Even if the feedforward event generator only transmits nine measurements of the disturbance [the red circles in Figure 14(a)], it performs equally well to the continuous-time feedforward control (green). Further discussion on the design of feedforward, event-based control is given in [20].

Now consider the case when there are no disturbances:  $d(t) = 0$  for all  $t \geq 0$ . The system in Figure 13 is a conventional event-based PI control system studied by many authors in [21]–[27]. Some of these works [23], [24], [26] investigate event-based PI control with events generated when the measurement error reaches above a threshold  $\bar{e}$

$$|y(t) - y(t_k)| \geq \bar{e}.$$

In [23] and [24], the performance of the PI controller with this sampling scheme was evaluated in industrial control loops at the Iggesund Mill. It was demonstrated that, with a careful selection of the threshold, the sampling may be reduced as much as 90% or more with only a marginal loss of control performance. Figure 15 [which is redrawn from Figure 3 in (24)] shows step responses for a reject tank.

In Table 3, the results are summarized for three performance measures: integrated absolute control error, integrated squared control error, and average overshoot for the negative and positive steps. The table also gives the communication reduction percentage relative to fast periodic control. More advanced setpoint tracking for event-based

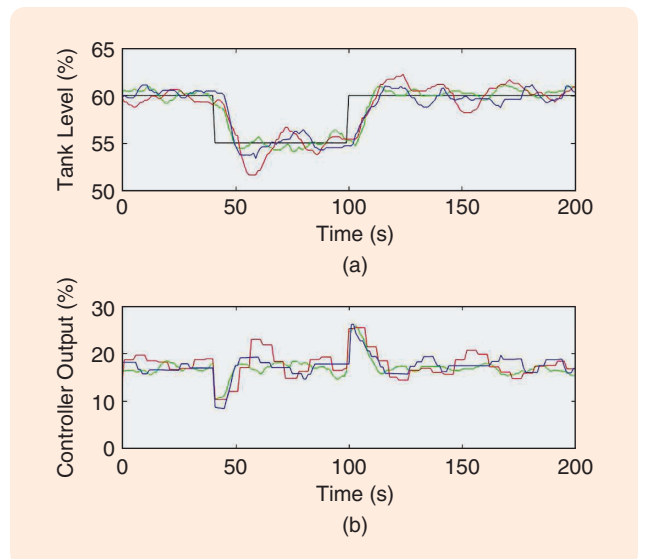


**FIGURE 15** Step responses on the reject tank process at Iggesund for three sampling schemes: fast periodic,  $h = 0.5$ [s] (green), slow periodic,  $h = 5$ [s] (red), and event-based  $\bar{e} = 0.5$ [s] (blue) control. The event-based control still has a similar performance compared to fast periodic, despite an almost 90% communication reduction. See also Table 3.

PI control was developed in [27] by modifying the event-based PIDPLUS [28]. An interesting topic for further study is the combination of event-based sampling for the various sensors in other control architectures in addition to feedback and feedforward configurations.

### PROOF-OF-CONCEPT IMPLEMENTATION AT IGGESUND PAPERBOARD

This section presents a proof-of-concept implementation at the Iggesund paper mill in the process section introduced in “The Iggesund Paperboard Machine Case Study” section. The part of the starch cooking section that was used for the field trials is illustrated in Figure 16. The starch is produced in batches. A batch is started when the level of the storage tank reaches a predefined low threshold value and stopped when the level of the storage tank reaches the high threshold value. During the week when the starch cooking process was controlled, the production rate was set to 1500 kg/h. A typical batch ran for approximately 1 h and was stopped for 23 h, depending on the quality of the paperboard produced.

A separate process controller was installed in parallel with the existing control system, should any failures during the experiments arise. The control loops were closed using both wireless sensors ( $S_4, S_5, S_6$ ) and wireless actuators ( $A_4, A_5, A_6$ ), as in Figure 16. The control loops were

implemented in the ABB AC800M controller using standard proportional-integral-derivative (PID) controllers with the same control parameters as the existing control system.

The wireless system was equipped with a deterministic failure detection feature. Therefore, the additional process controller would be able to signal to the normal control system to take over in the event of a detected error. The wireless actuators would also detect such an error at the same time as the other communication peers in the system, thus being able to electrically switch back the control of the valves to the normal control system. This may seem ambitious to implement such functionality to conduct

**TABLE 3** Step response performances of three sampling schemes for the reject tank: fast periodic (FP)  $h = 0.5$  s, slow periodic (SP)  $h = 5$  s, and event based (EB)  $\bar{e} = 0.5$ . The performance is evaluated through communication reduction (CR) and the three measures: integrated absolute control error, integrated squared control error, and overshoot (OS).

Scheme	CR%	$\int  e(t) $	$\int  e(t) ^2$	OS%
FP	0	141.3	295.9	15.0
SP	90.0	229.7	486.2	53.7
EB	87.9	174.9	392.1	22.5

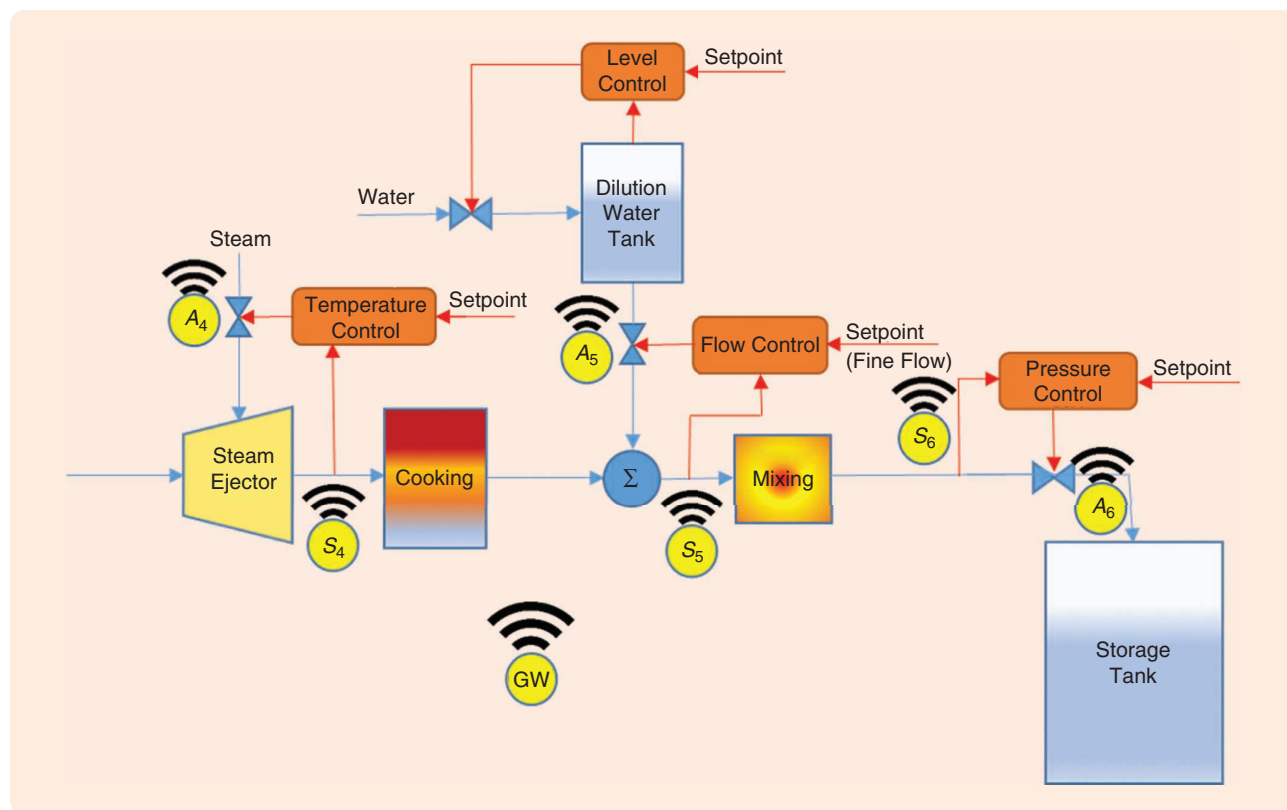


**FIGURE 16** A block diagram of a starch cooker. Three control loops are installed with wireless actuators and wireless sensors. The level controller is a proportional-integral (PI) controller, the temperature controller is also a PI controller, and the pressure controller is a proportional-integral-derivative controller. GW: gateway.

## A standard choice for the DCNs and other intelligent devices would be to use wireless communications.

experiments for research. However, it was required to conduct measurements and control 24 h per day for five calendar days without manually restoring production in the event of a failure.

The additional process controller (AC800M from ABB) was connected to a GW in the process via Profinet IO, using an existing fiber between the process and the marshalling

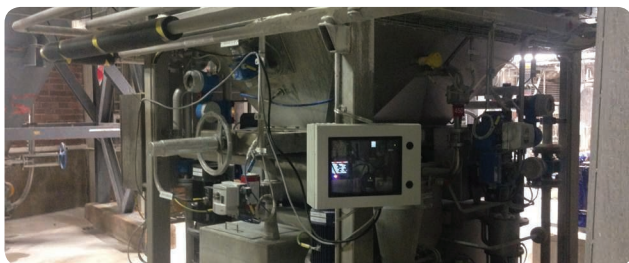


**FIGURE 17** The environment where the wireless devices were installed. A mixing tank is shown where the flow of the slurry into the cooking process is measured. The gateway and the field devices were realized by assembling two off-the-shelf evaluation boards in an IP67 enclosure. A controller area network bus input–output from ABB (CI581) with analog inputs and outputs as well as digital counterparts, was connected to the field devices.

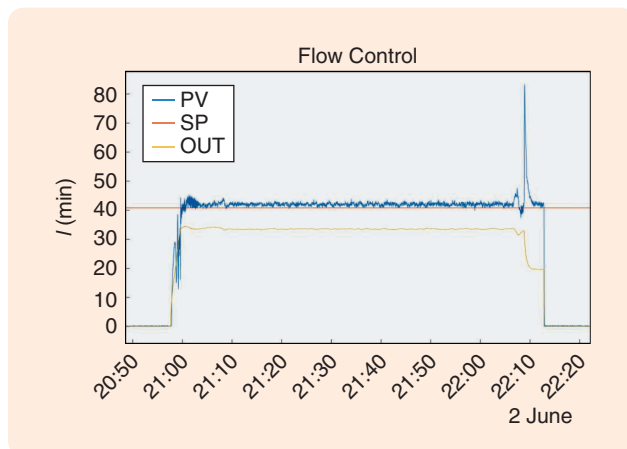


**FIGURE 18** The performance of the flow controller during the starch cooking process. PV is the process value in L/min, SP is the setpoint, and OUT is the output signal to the control valve (percentage). At the beginning of the batch sequence at 21:00, the flow controller aims to keep a water flow of 41 L/min. Shortly before 22:10, the level of the storage tank has reached the upper threshold, the control valves to the storage tanks are closed, and a cleaning process starts. The opening of the pressure valve (see Figure 19) for cleaning acts as a flow disturbance. The cleaning process finishes at 22:15, and the starch cooking system is ready for another batch as soon as the storage tank level reaches its lower threshold.

room where the control equipment was installed. In the process, the wireless instruments and the wireless actuators were installed and connected to the existing valves and instrumentation using four 20-mA interfaces. The GW and the field devices were realized by assembling two off-the-shelf evaluation boards in an IP67 enclosure, as shown in Figure 17.

Challenges with existing industrial WSN standards (WirelessHART or ISA100) for wireless control were previously identified [29]. Therefore, solutions to overcome limitations were proposed and implemented, including real-time uplinks, seamless recovery in the event of link failures, and diagnostics to take the end nodes into a safe state in a timely manner in the event of communication errors. One solution is Realflow [30] (which was used in this proof-of-concept implementation) as well as a new time synchronization protocol [31] with more precise time-division media access. In addition, solutions to enable several concurrent data flows with different priorities were implemented for a deterministic communication network supporting online and topology changes without any deadline misses in the real-time communication paths, which is required for control applications.

Consider the flow control depicted in Figure 18. In the beginning of the batch sequence (just before 21:00), the flow controller is enabled to keep a water flow of 41 L/min. At this moment, the control valve of the pressure controller is opened to 50% to flush out the remaining starch from the previous batch, as shown in Figure 19. In parallel with starting the heating of the boiler, the pressure controller is enabled to maintain a pressure of 3.3 bar in the boiler. The batch sequence then enables a ramp in the output of the control valve to heat the boiler with steam. When the temperature of the boiler is close to its setpoint of 138 °C, the temperature controller is enabled to maintain the temperature. This can be seen in Figure 20 by the “knee” in the yellow line some minutes after 21:00.

Just before 22:10, the level of the storage tank has reached the upper threshold, the control valves to the storage tanks are closed, and a cleaning process starts. In Figure 18, a flow disturbance is noticed when the pressure valve is opened for cleaning (see Figure 19). The cleaning process finishes at 22:15, and the starch cooking system is ready for another batch when the storage tank level reaches its lower threshold.

The batch sequence began approximately every third hour during the five-day experiment period. During this period, the plant operators could neither identify any significant

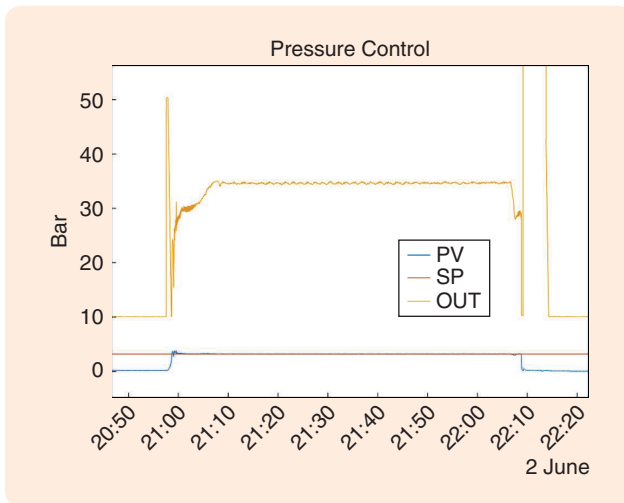


**FIGURE 19** The performance of the pressure controller during the starch cooking process. PV is the process value (in bars), SP is the setpoint, and OUT is the output signal to the control valve (percentage). At the beginning of the batch process at 21:00, the control valve of the pressure controller is opened to 50% to flush out the starch remaining from the previous batch. The pressure controller then aims to maintain a pressure of 3.3 bars while heating the boiler (see Figure 20). Once the batch process is completed (just before 22:10), the cleaning process starts by opening the pressure valve and finishes at 22:15.

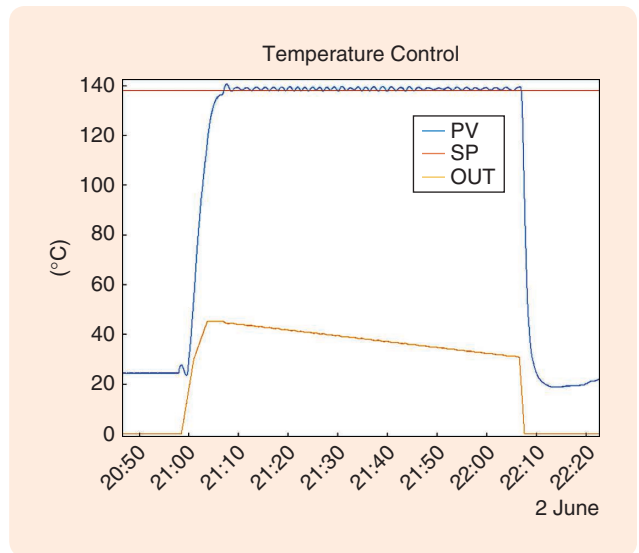


**FIGURE 20** The performance of the temperature controller during the starch cooking process. PV is the process value in degrees Celsius, SP is the setpoint, and OUT is the output signal to the control valve (percentage). At the beginning of the batch process (around 21:00), the boiler starts to heat with steam using a ramp in the output of the control valve. When reaching the desired temperature of 138 °C (shortly after 21:00), the temperature controller is enabled to maintain the temperature.

differences between the wireless and Profibus-controlled process nor did the production system detect any deviations with respect to the control limits installed to provide early warning that the process section was in need of maintenance. In addition, the safety functionality that restores operation to the normal production system was never invoked since there were no three consecutive communication errors during the five-day period. Even when comparing production data between the wireless and normally controlled process, no differences could be discerned. However, slightly different variations were observed in the final concentration of the starch. The operators noted that they could see such variations occasionally in the normal production system, and the variations were explained by differences in the density of the ingredients in the storage tank before mixing. This implies that the feeders' duty cycle will feed a small variation in volume of the ingredients, which varies over time depending on how full the tank is.

Overall, the operators and the automation engineers concluded that they could not tell if the process was controlled with a wireless or wired technology. Due to the inherent variations in the quality of the process ingredients, the difference in control performance between the wireless and Profibus-controlled process could not be quantified. However, our experiments indicate that it is feasible to design and implement wireless systems for process control, and there is no need to treat them differently than the wired control counterparts or from a quality control performance perspective. Furthermore, our wireless

control experiment indicates that it is feasible to use wireless control for continuous operation and production. From an availability perspective, this is too short a time to draw any general conclusions. However, comparing the performance indicators from the wireless installation with the same indicators using the Profibus network suggests that it would be possible to reach the desired availability with a wireless installation.

## CONCLUSIONS

This article presents important research problems that are critical to solve before deploying wireless control systems in process industries. In large industrial plants (as with a paper mill), information from thousands of sensors would then have to be handled swiftly over wireless links. We have addressed the importance of a correct characterization of the radio environment, the use of suitable network protocols for routing sensor information to the GWs, the efficient use of harvested energy from the environment, and the use of robust (possibly event-based) and reconfigurable control algorithms. Furthermore, we deployed a wireless networked control system addressing these aspects at Iggesund Paperboard. Long-term tests were conducted on one of the mill's starch cookers during normal production over five consecutive days. The tests were very successful, and the operators could not distinguish the wireless control system from the wired, which suggests that it is indeed possible to replace wired control systems with wireless ones, even in a complex industrial environment.

## From a system perspective, there are also several challenges to maintain high availability and safe control functions.

### ACKNOWLEDGMENTS

This work was supported by VINNOVA, The Swedish Governmental Agency for Innovation Systems. The authors thank Piyush Agrawal, Subhrakanti Dey, Mikael Gidlund, Ewa Hansen, Jonas Neander, Tommy Norgren, Tomas Olofsson, Jonathan Styrud, and Junfeng Wu for their helpful suggestions and Iggesund Paperboard for allowing us to conduct radio-channel measurements and wireless control tests on the paper mill's starch cooker during normal production.

### AUTHOR INFORMATION

**Anders Ahlén** (anders.ahlen@signal.uu.se) is a professor and chair of signal processing at Uppsala University, Sweden, where he is the head of the Signals and Systems Division of the Department of Engineering Sciences. He received the Ph.D. degree in automatic control from Uppsala University. He was with the Systems and Control Group at Uppsala University from 1984 to 1992 as an assistant and associate professor in automatic control. In 1991, he was a visiting researcher in the Department of Electrical and Computer Engineering at the University of Newcastle, Australia, and he has been a visiting professor there several times since 2008. From 2001 to 2004, he was the chief executive officer of Dirac Research AB, a company offering state-of-the-art audio signal processing solutions, where he has been the chair of the board of directors since 2005. His research interests include signal processing and communications and control, with a current focus on signal processing for wireless communications, wireless sensor networks, wireless control, and audio signal processing. From 1998 to 2004 he was the editor of signal and modulation design for *IEEE Transactions on Communications*. He is a Senior Member of the IEEE and a member of the Royal Society of Sciences at Uppsala.

**Johan Åkerberg** is a principal scientist at ABB Corporate Research, Västerås, Sweden. He received the M.Sc. and Ph.D. degrees in computer science and engineering from Mälardalen University, Sweden. He has 25 years of experience with ABB in various positions, such as the global research area coordinator, research and development project manager, automation lead engineer, industrial communication specialist, and product manager.

**Markus Eriksson** received the Ph.D. in electrical engineering from Uppsala University, Sweden, in 2019. He was a software developer at Scania CV in Södertälje, Sweden. His research interests are in signal processing, specifically, in change point detection and embedded systems.

**Alf J. Isaksson** received the M.Sc. degree in computer engineering and the Ph.D. degree in automatic control, both

from Linköping University, Sweden, in 1983 and 1988, respectively. After graduating, he was an assistant professor at Linköping University until 1991. From 1991 to 1992, he was a research associate at the University of Newcastle, Australia. In 1992, he joined the Royal Institute of Technology, Stockholm, where he was promoted to professor in 1999. In 2001, he made the shift from academic to industrial research and joined ABB Corporate Research, Västerås, Sweden. He became a corporate research fellow in 2009 and has been the group research area manager since 2014, where he is responsible for internally funding all research in control at ABB's seven research centers. He was also an adjunct professor in automatic control at Linköping University from 2006 to 2015, where he led the Process Industry Center from 2009 to 2012. He is currently creating ABB Future Labs, which focuses on artificial intelligence and autonomous systems. He is a Senior Member of the IEEE and a member of the Royal Swedish Academy of Engineering Sciences.

**Takuya Iwaki** received the B.E. and M.E. degrees from the Tokyo Institute of Technology, Japan, in 2009 and 2012, respectively. He was with JGC Corporation, Yokohama, Japan, as a process control engineer from 2012 to 2016. He is currently a Ph.D. student in the School of Electrical Engineering and Computer Science, KTH Royal Institute of Technology, Stockholm, Sweden. His main research interests include control and estimation over wireless communication and their application to industrial process control systems.

**Karl Henrik Johansson** is a professor in the School of Electrical Engineering and Computer Science, KTH Royal Institute of Technology, Stockholm, Sweden. He received the M.Sc. and Ph.D. degrees from Lund University. He has held visiting positions at the University of California Berkeley, Caltech, Nanyang Technological University Singapore, Hong Kong University of Science and Technology Institute of Advanced Studies, and the Norwegian University of Science and Technology. His research interests are in networked control systems; cyberphysical systems; and applications in transportation, energy, and automation networks. He has served on the IEEE Control Systems Society Board of Governors, the IFAC Executive Board, and the European Control Association Council. He has received several best paper awards and other distinctions from the IEEE and Association for Computing Machinery. He has been awarded a Distinguished Professor with the Swedish Research Council and Wallenberg Scholar with the Knut and Alice Wallenberg Foundation. He received the Future Research Leader Award from the Swedish Foundation for Strategic Research

and the triennial IFAC Young Author Prize. He is a Fellow of the IEEE and the Royal Swedish Academy of Engineering Sciences, and he is an IEEE Distinguished Lecturer.

**Steffi Knorn** received the Dipl.-Ing. degree in 2008 from the University of Magdeburg, Germany, and the Ph.D. degree from the Hamilton Institute at the National University of Ireland Maynooth, Ireland, in 2013. In 2013, she was a research academic at the Centre for Complex Dynamic Systems and Control at the University of Newcastle, Australia. Since 2014, she has been with the Signals and Systems Division at Uppsala University, Sweden. Her research interests include stability analysis and controller design for marginally stable two-dimensional systems, port-Hamiltonian systems, string stability and scalability of vehicle platoons, distributed control, multisensor estimation, and energy harvesting and energy sharing in wireless networks.

**Thomas Lindh** is an automation engineer for Maintenance Technology Development, Iggesund Mill, Iggesund Paperboard, Sweden. He has 20 years of experience in the pulp and paper industry. He was an instrument technician for nine years and has been an automation engineer for the last 11. He is the system administrator for the distributed control system at the board machines.

**Henrik Sandberg** is a professor in the Division of Decision and Control Systems, KTH Royal Institute of Technology, Stockholm, Sweden. He received the M.Sc. degree in engineering physics and the Ph.D. degree in automatic control from Lund University, Sweden, in 1999 and 2004, respectively. From 2005 to 2007, he was a postdoctoral researcher at the California Institute of Technology, Pasadena. In 2013, he was a visiting scholar in the Laboratory for Information and Decision Systems, Massachusetts Institute of Technology, Cambridge. He has also held visiting appointments at the Australian National University and the University of Melbourne, Australia. His current research interests include the security of cyberphysical systems, power systems, model reduction, and fundamental limitations in control. He received the Best Student Paper Award from the 2004 IEEE Conference on Decision and Control, the 2007 Ingvar Carlsson Award from the Swedish Foundation for Strategic Research, and a Consolidator Grant from the Swedish Research Council in 2016. He has served on the editorial board of *IEEE Transactions on Automatic Control* and is an associate editor of *Automatica*.

## REFERENCES

- [1] T. S. Rappaport and C. D. McGillem, "UHF fading in factories," *IEEE J. Sel. Areas Commun.*, vol. 7, no. 1, pp. 40–48, 1989.
- [2] A. Willig, "Recent and emerging topics in wireless industrial communication," *IEEE Trans. Ind. Informat.*, vol. 4, no. 2, pp. 102–124, 2008.
- [3] P. Antsaklis and J. Baillieul, "Special issue on technology of networked control systems," *Proc. IEEE*, vol. 95, no. 1, pp. 5–8, 2007.
- [4] J. P. Hespanha, P. Naghshtabrizi, and Y. Xu, "A survey of recent results in networked control systems," *Proc. IEEE*, vol. 95, no. 1, pp. 138–162, 2007.
- [5] P. Park, S. Coleri Ergen, C. Fischione, C. Lu, and K. H. Johansson, "Wireless network design for control systems: A survey," *IEEE Commun. Surveys Tuts.*, vol. 20, no. 2, pp. 978–1013, 2018.

- [6] H. Forbes, *ExxonMobil's Quest for the Future of Process Automation*. Dedham MA: ARC Insights, ARC Advisory Group, 2016.
- [7] D. Clark, "The IoT of automation—A totally new way to look at control and automation in the process industries," in *Proc. LCCC Workshop Process Control*, Department of Automatic Control, Lund Institute of Technology, Lund University, 2016.
- [8] I. F. Akyildiz, W. Su, Y. Sankarasubramaniam, and E. Cayirci, "Wireless sensor networks: A survey," *Comput. Netw.*, vol. 38, no. 4, pp. 393–422, 2002.
- [9] V. C. Gungor and G. P. Hancke, "Industrial wireless sensor networks: Challenges, design principles, and technical approaches," *IEEE Trans. Ind. Electron.*, vol. 56, no. 10, pp. 4258–4265, 2009.
- [10] T. S. Rappaport, *Wireless Communication: Principles and Practice*, 2nd ed. New Jersey: Prentice Hall PTR, 1996.
- [11] H. Hashemi, M. McGuire, T. Vlasschaert, and D. Tholl, "Measurements and modeling of temporal variations of the indoor radio propagation channel," *IEEE Trans. Veh. Technol.*, vol. 43, no. 3, pp. 733–737, 1994.
- [12] T. S. Rappaport, "Characterization of UHF multipath radio channels in factory buildings," *IEEE Trans. Antennas Propag.*, vol. 37, no. 8, pp. 1058–1069, 1989.
- [13] H. Hashemi, "The indoor radio propagation channel," *Proc. IEEE*, vol. 81, no. 7, pp. 943–968, July 1993.
- [14] R. Bultitude, "Measurement, characterization and modeling of indoor 800/900 MHz radio channels for digital communications," *IEEE Commun. Mag.*, vol. 25, no. 6, pp. 5–12, 1987.
- [15] P. Agrawal, A. Ahlén, T. Olofsson, and M. Gidlund, "Long term channel characterization for energy efficient transmission in industrial environments," *IEEE Trans. Commun.*, vol. 62, no. 8, pp. 3004–3014, 2014.
- [16] T. Olofsson, A. Ahlén, and M. Gidlund, "Modeling of the fading statistics of wireless sensor network channels in industrial environments," *IEEE Trans. Signal Process.*, vol. 64, no. 12, pp. 3021–3034, 2016.
- [17] M. Masdari and M. Tanabi, "Multipath routing protocols in wireless sensor networks: A survey and analysis," *Int. J. Future Gen. Commun. Netw.*, vol. 6, no. 6, pp. 181–192, 2013.
- [18] L. Rabiner, "A tutorial on hidden Markov models and selected applications in speech recognition," *Proc. IEEE*, vol. 77, no. 2, pp. 257–286, Feb. 1989.
- [19] C. K. Ho, P. D. Khoa, and P. C. Ming, "Markovian models for harvested energy in wireless communications," in *Proc. IEEE Int. Conf. Communication Systems*, 2010. doi: 10.1109/ICCS.2010.5686445.
- [20] T. Iwaki, J. Wu, and K. H. Johansson, "Event-triggered feedforward control subject to actuator saturation for disturbance compensation," in *Proc. European Control Conf.*, 2018, pp. 501–506.
- [21] K.-E. Årzén, "A simple event-based PID controller," in *Proc. IFAC World Congr.*, 1999, vol. 18, pp. 423–428.
- [22] M. Rabi and K. H. Johansson, "Event-triggered strategies for industrial control over wireless networks," in *Proc. Int. Conf. Wireless Internet*, 2008, pp. 1–7.
- [23] T. Norgren and J. Styruud, "Non-periodic sampling schemes for control applications," Master's thesis, Uppsala Univ., 2011.
- [24] T. Norgren, J. Styruud, A. J. Isaksson, J. Åkerberg, and T. Lindh, "Industrial evaluation of process control using non-periodic sampling," in *Proc. IEEE Conf. Emerging Technologies and Factory Automation*, 2012, pp. 1–8.
- [25] C.-F. Lindberg and A. J. Isaksson, "Comparison of different sampling schemes for wireless control subject to packet losses," in *Proc. Int. Conf. Event-Based Control, Communication, and Signal Processing*, 2015, pp. 1–8.
- [26] G. A. Kiener, D. Lehmann, and K. H. Johansson, "Actuator saturation and anti-windup compensation in event-triggered control," *Discrete Event Dyn. Syst.*, vol. 24, no. 2, pp. 173–197, 2014.
- [27] U. Tiberi, J. Araújo, and K. H. Johansson, "On event-based PI control of first-order processes," in *Proc. IFAC Conf. Advances in PID Control*, 2012, pp. 448–453.
- [28] T. Blevins, D. Chen, M. Nixon, and W. Wojsznis, *Wireless Control Foundation: Continuous and Discrete Control for the Process Industry*. Research Triangle Park, NC: International Society of Automation, 2015.
- [29] J. Åkerberg, M. Gidlund, and M. Björkman, "Future research challenges in wireless sensor and actuator networks targeting industrial automation," in *Proc. IEEE Int. Conf. Industrial Informatics*, 2011, pp. 410–415.
- [30] K. Yu, Z. Pang, M. Gidlund, J. Åkerberg, and M. Björkman, "Real-flow: Reliable real-time flooding-based routing protocol for industrial wireless sensor networks," *Int. J. Distrib. Sens. N.*, vol. 10, no. 7, pp. 1–17, 2014. doi: 10.1155/2014/936379.
- [31] T. Lennvall, J. Åkerberg, E. Hansen, and K. Yu, "A new wireless sensor network TDMA timing synchronization protocol," in *Proc. IEEE Int. Conf. Industrial Informatics*, 2016, pp. 606–611.